REVIEWS OF TOPICAL PROBLEMS

Low energy methods of molecular laser isotope separation

Physics – Uspekhi **58** (7) 670 – 700 (2015)

REVIEWS OF TOPICAL PROBLEMS PACS numbers: 07.77.Gx, **33.80. – b**, **36.40. – c**, **42.62. – b**, 42.62.Fi, 82.40.Fp, 82.50.Bc

Low energy methods of molecular laser isotope separation

G N Makarov

DOI: 10.3367/UFNe.0185.201507b.0717

Contents

Abstract. Of the many proposals to date for laser-assisted isotope separation methods, isotope-selective infrared (IR) multiphoton dissociation (MPD) of molecules has been the most fully developed. This concept served as the basis for the development and operation of the carbon isotope separation facility in Kaliningrad, Russia. The extension of this method to heavy elements, including uranium, is hindered by, among other factors, the high power consumption and the lack of high-efficiency high-power laser systems. In this connection, research and development covering low energy methods for the laser separation of isotopes (including those of heavy atoms) is currently in high demand. This paper reviews approaches to the realization of IR-laser-induced isotope-selective processes, some of which are potentially the basis on which low-energy methods for molecular laser isotope separation can be developed. The basic physics and chemistry, application potential, and strengths and weaknesses of these approaches are discussed. Potentially promising alternatives to the title methods are examined.

Keywords: atoms, molecules, clusters, molecular and cluster beams, laser spectroscopy, laser-induced selective processes, laser isotope separation

G N Makarov Institute of Spectroscopy, Russian Academy of Sciences, ul. Fizicheskaya 5, 142190 Troitsk, Moscow, Russian Federation
E-mail: gmakarov@isan.troitsk.ru

Received 27 February 2015, revised 21 April 2015
Uspekhi Fizicheskikh Nauk **185** (7) 717 – 751 (2015)
DOI: 10.3367/UFNr.0185.201507b.0717
Translated by Yu V Morozov; edited by A Radzig

1. Introduction

Isotopes of chemical elements find wide application in many areas of science and practice, such as chemistry, biology, medicine, nuclear power engineering, and other branches of industry [1]. In chemistry, stable isotopes are exploited for studying mechanisms of chemical reactions, synthesis of chemical elements, and catalysis. Such isotopes as ^{13}C and ^{18}O are used in medicine to diagnose a variety of diseases. Silicon is extensively employed to manufacture semiconductors. The demands for silicon, carbon, oxygen, and nitrogen

isotopes increase year by year. The ever-growing needs for stable isotopes are stimulating the search for new high-efficiency cost-effective methods of separating them.

The recent advent of laser sources generating radiation in a wavelength range from 0.2 to 20 μm has made it possible to extensively study techniques for laser-assisted isotope separation. The method based on selective multiphoton dissociation (MPD) of molecules by intense infrared (IR) radiation is considered to be especially promising for the separation of medium-mass isotopes. An advantage of this technique is the employment of pulsed CO_2 lasers as radiation sources operating at a pulse repetition rate up to about 400–500 Hz and a mean radiation power of several kilowatts with an efficiency of 5–10%. Moreover, CO_2 lasers are rather simple to operate and relatively inexpensive. The method was implemented to separate carbon isotopes under practical conditions. A plant for separating ^{13}C isotopes based on selective MPD of CF_2HCl (Freon-22) molecules by a pulse-periodic CO_2 laser [1–7] has recently been commissioned and successfully operated in the city of Kaliningrad, Russia.

The worldwide boom in nuclear power engineering dictates the high demand currently for enriched uranium. To-day, gas diffusion and gas centrifugation with the use of uranium hexafluoride (UF_6) as the starting material are the main methods for commercial uranium enrichment. These techniques take advantage of the difference between the masses of depleted uranium-238 and fissionable uranium-235 isotopes. Laser-assisted separation of uranium isotopes is based on the difference in the spectra of laser radiation absorption either by isotopes of atomic uranium (atomic vapor laser isotope separation, AVLIS) [8, 9] or by isotopomers of uranium hexafluoride (molecular laser isotope separation, MLIS, and separation of isotopes by laser excitation, SILEX) [10, 11].

In the 1970s, serious attempts were undertaken in the USA to develop effective laser systems for uranium isotope separation on a large scale. However, it proved impossible to overcome technical difficulties, and the work was practically stopped. In the same period, attempts to design more cost-effective methods for uranium enrichment than the traditional gas diffusion technique were made in some other countries (UK, Germany, France, RSA, Japan). The latter method is currently falling into disuse due to the high energy expenditure. Most of these projects were also shut down in the late 1990s.

At present, the building of four new uranium enrichment facilities is underway in the USA. Three of them are designed to employ promising centrifuge technologies, whereas laser-assisted enrichment based on the SILEX technique will be used in the fourth (see Section 9).

The development of a method for molecular laser separation of isotopes (including those of heavy elements) based on IR MPD [12–17] is hampered by high power consumption (around 40–50 quanta of IR radiation with a wavelength of 16 μm, i.e. 3.5-4.5 eV of energy, need to be absorbed to dissociate a UF_6 molecule), the lack of high-efficiency high-power laser systems, and a variety of other factors. The high power consumption of the process is responsible for its low effectiveness compared with that of the traditional centrifugation technique. The lack of high-efficiency high-power tuned laser systems operating in a wavelength range of 16 μm hinders applications of isotope-selective IR MPD of UF_6 molecules. Nevertheless, such work is still underway (see, e.g., Refs [18–20]); hence, the importance of research designed to develop low-energy methods (LEMs) of molecular laser isotope separation (MLIS), including the separation of heavy element isotopes. For the purpose of LEMs, the activation energy must be $\leqslant 1$ eV. Such energies are characteristic of physicochemical processes of molecule adsorption and desorption on a solid surface, and possibly coated with molecules or clusters, and on the surface of large clusters. Also, such activation energies are needed for the dissociation and fragmentation of weakly bound van der Waals molecules.

The present review highlights various approaches to the realization of isotope-selective processes induced by IR laser radiation. Some of them are expected to serve as the basis for the development of low-energy methods of molecular laser isotope separation. The paper outline is as follows.

Section 2 describes results of earlier isotope separation experiments making use of heterogeneous surface processes induced by continuous CO_2 lasers.

Section 3 is focused on isotope-selective IR laser vibrational predissociation of van der Waals molecules.

The method for selective control of molecular condensation in gas-dynamically cooled jets and flows using IR laser radiation is discussed in Section 4.

Section 5 describes the isotope separation technique based on low-energy electron capture by molecules.

Selection of molecules embedded in nanodroplets (clusters) of superfluid helium is considered in Section 6.

The results of laser-driven experiments on the interaction of vibrationally highly excited and unexcited molecules with molecules (clusters) condensed on a cold surface are presented and analyzed in Section 7.

Section 8 is devoted to the isotope separation technique with the participation of clusters and nanoparticles.

Section 9 presents some facts about the SILEX Company and its technology.

Section 10 contains a concise analysis of the method for isotope-selective infrared multiphoton dissociation of molecules under nonequilibrium conditions of a pulsed gas-dynamically cooled molecular flow interacting with a solid surface. It is the author's opinion that this method may be a promising alternative to low-energy methods of molecular laser isotope separation.

Concluding Section 11 summarizes the results of research reviewed in this report along with the most important achievements of and prospects for molecular laser isotope separation.

2. Heterogeneous molecular laser isotope separation

2.1 Basis of the method and proposed models

Methods for molecule selection based on heterogeneous processes accompanying the interaction of molecules with a cold surface were proposed in the early period of IR laser application to isotope separation. These methods make use of the difference between probabilities of physical adsorption (or desorption) processes involving excited and unexcited molecules on a cold surface covered with a condensed-phase layer of incident molecules. In the case of physical adsorption, the adsorption E_{ad} and desorption E_{des} energies are equal: $E_{ad} = E_{des}$ [21]. Adsorption energies of molecules on a molecule (cluster)-coated surface are commensurate with van der Waals interaction energies (0.1–0.5 eV) [22], i.e.,

they are much lower than the molecular dissociation energy ($\approx 3-5$ eV) [23]. For this reason, selective heterogeneous adsorption and desorption processes are of great interest in the context of developing the low-energy methods for molecular laser separation.

Theoretical and experimental studies of the molecular condensation on a cold surface depending on their internal energy are reported in Refs [24–27] and [27–29], respectively. A variety of mechanisms responsible for different surface adhesion (adsorption) coefficients of vibrationally excited and unexcited molecules have been postulated. By way of example, the authors of Ref. [24] supposed that the surface adhesion coefficient S of polyatomic molecules can be expressed through the relation

$$S = 1 - \exp\left(-\frac{E_{\rm ad}}{E_{\rm tot}}\right), \tag{2.1}$$

where $E_{\rm tot}$ is the total energy of the incident molecule, i.e., the sum of translational $E_{\rm trans}$, vibrational $E_{\rm vib}$, and rotational $E_{\rm rot}$ energies:

$$E_{\rm tot} = E_{\rm trans} + E_{\rm vib} + E_{\rm rot}\,. \tag{2.2}$$

It follows from relation (2.1) that, due to the difference between surface adhesion coefficients (and consequently reflection) of selectively excited and unexcited molecules, they can be selected based on their isotope and (or) component composition. It is clear, however, that this model makes possible only a highly simplified description of complicated molecule–surface interactions.

It was argued in Ref. [27] that the local heating of phonons by energy $E_{\rm tot}$ transferred by an adsorbed particle may cause evaporation of the molecule from the surface. However, such a description of condensation and evaporation processes is not quite correct. It was suggested in Ref. [25] that an enhanced probability of excited molecule reflection from a surface should be critically dependent on the efficiency of vibrational–translational (V–T) relaxation, i.e., the conversion of vibrational into translational energy during collisions of molecules with the surface. The authors of Ref. [26] proposed a phenomenological model for the description of the influence of the molecular internal energy on condensation that implies that rotational and low-frequency vibrational excitations have a marked effect on the molecule adhesion coefficient.

2.2 Experimental results

All the models mentioned in Section 2.1 do predict, despite being simplified, that the excitation of molecular internal degrees of freedom must interfere with condensation. Experiments have yielded contradictory data as regards the influence of the internal energy of molecules on physical adsorption processes. References [27, 28] (see also review [29]) describe experiments with CO and CO_2 molecules excited in an electric discharge [27] and with BCl_3 molecules excited by laser radiation [28]; the results demonstrated a rather strong dependence of the molecule condensation rate on vibrational temperature. However, later studies [30] failed either to reproduce the results of paper [28] or to observe any appreciable effect of the internal energy of laser-excited BCl_3 molecules on condensation. At the same time, the authors of Ref. [30] do not altogether rule out the influence of vibrational energy on condensation rate.

The influence of vibrational and translational energies of molecules on the probability of condensation (adsorption) during their collisions with the condensed phase on a cold surface has been thoroughly investigated in Ref. [31] by the example of CCl_4 and SF_6 molecules and using an effusive molecular beam (see also Ref. [32]). The internal (vibrational and rotational) temperature of molecules in the beam was altered by varying the beam source temperature in a range from 300 to 700 K. This allowed generating molecular beams with different internal and translational energies and their different ratios. The temperature of the surface on which molecule condensation occurred was 50 K, and the probability of molecule adhesion to the surface amounted to no less than 99%, thus enabling the authors of Ref. [31] to detect molecules inelastically scattered from the surface.

It was shown [31] that the thermal excitation of vibrational and rotational degrees of freedom in the molecules may enhance the probability of their reflection from the surface, i.e., decrease the adhesion probability. The influence of the molecular internal energy on reflection probability is especially apparent in the case of a low incident velocity of the molecules and practically disappears at high velocities (Fig. 1a). In the low-velocity limit (around 2.7×10^4 cm s^{-1}), the so-called enrichment coefficient $K_{\rm enr}$ for CCl_4 and SF_6 molecules took roughly the values of 3.7 and 4.6, respectively (Fig. 1b). The enrichment coefficient $K_{\rm enr} = 4.6$ implies that SF_6 molecules with excited internal degrees of freedom and a mean velocity in the beam reaching 2.7×10^4 cm s^{-1} are reflected from a cool SF_6-coated surface with a probability 4.6 times that for vibrationally and rotationally 'cold' molecules. For a high incident velocity ($\geqslant 5.0 \times 10^4$ cm s^{-1}), the enrichment coefficient for both CCl_4 and SF_6 molecules tend toward unity. These results illustrate [31] the operating capacity of heterogeneous laser isotope separation schemes based on selective vibrational excitation of molecules. However, such schemes await further exploration.

The slow-down of molecule condensation in the presence of vibrational excitation was described for $^{235}UF_6$, too [33]. In these experiments, a 2.6-m long tubular cell placed inside the resonator of a CO laser at $-33\,^\circ$C was filled with a gaseous mixture of UF_6/HBr/Ar (1.5/20/20) under a total pressure of 41.5 Torr. The laser was tuned to a frequency range of 1876.3–1876.6 cm^{-1} to excite mostly the $3\nu_3$ vibrational mode of $^{235}UF_6$ molecules. The concentration of these molecules in the cell increased from 0.712% (natural content) to 0.727% (enrichment coefficient $K_{\rm enr} \approx 1.021$).

Separation of carbon isotopes by slowing down $CHCl_3$ condensation rate in a mixture with He or N_2 was investigated in Ref. [34]. This gaseous mixture was passed with a subsonic speed through a co-axial cylindrical chamber with cold walls and irradiated at a continuous CO_2-laser frequency modulated in the range of 934.9–929.0 cm^{-1}. It was established that the desorption probability of vibrationally excited molecules from the cold walls is higher than that of unexcited molecules. Specifically, the concentration of excited molecules in the gaseous phase of a $CHCl_3$/nitrogen mixture in the chamber was 15% higher than in a natural isotopomer mixture. Under the selective vibrational excitation of molecules, $^{12}CHCl_3$ and $^{13}CHCl_3$ isotopomers were separated with an enrichment coefficient from 1.01 to 1.15. Irradiation of a $CHCl_3$/helium mixture failed to cause separation.

To sum up, we considered in the present section selective heterogeneous processes that occur when molecules are excited by continuous CO_2 lasers, and the excitation of their

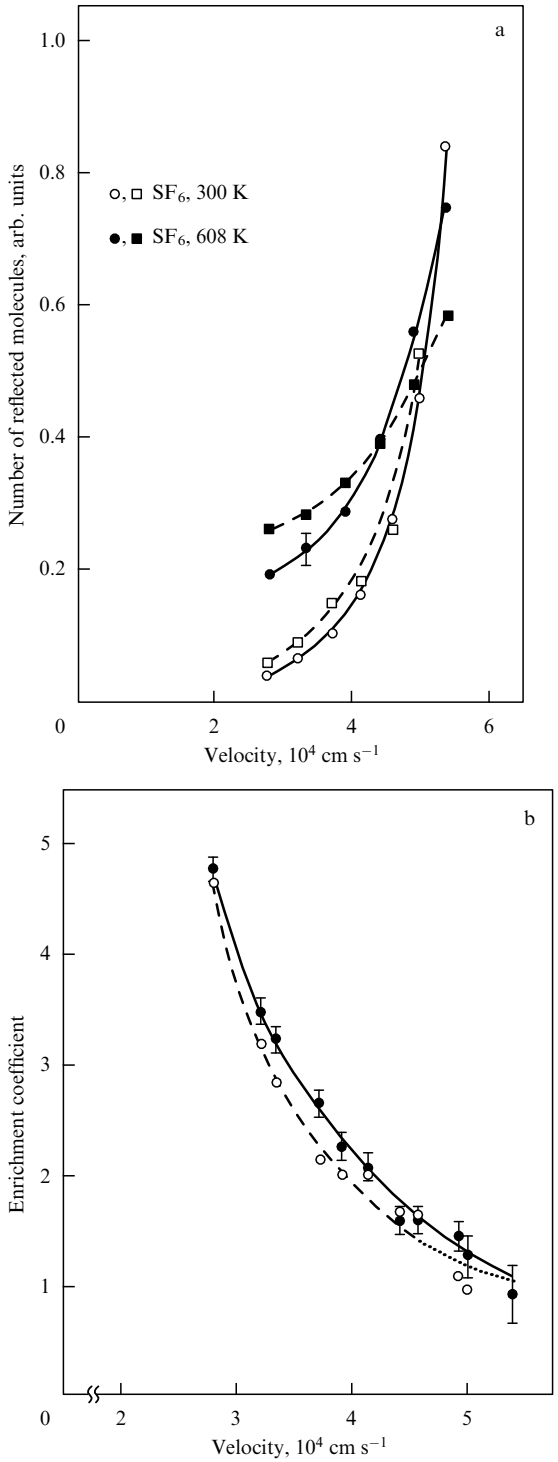

Figure 1. (a) Probability of SF_6-molecule reflection from the surface versus the incident velocity at the gas temperature above the nozzle $T_0 = 300$ and 608 K. Dashed curves and squares indicate the probability of molecular reflection, taking account of the finite width of the modulator-specified molecular velocity distribution in the beam [31]. (b) Enrichment coefficient of SF_6 molecules determined by their internal energy as a function of incident velocity of molecules. Dashed curves and circles show variations of the enrichment coefficients, taking into account the finite width of molecular velocity distribution in the beam. Dotted curve demonstrates the approximation of this dependence over a velocity interval of around $(4.5-5.5)\times 10^4$ cm s^{-1} [31].

high vibrational states is unlikely. Most excited molecules moved to the first vibrational level with an energy of ~ 0.12 eV. Similar experiments with the employment of high-power pulsed CO_2 lasers to excite molecules and cause their transition to higher vibrational states are described in Section 7.

3. Selective infrared vibrational predissociation of van der Waals molecules

3.1 Physical foundation of the method

One of the approaches to the realization of LEM MLIS is based on the method of IR vibrational predissociation of weakly bound van der Waals molecules, in particular, dimers. This method was proposed at the early stages of the development of laser-assisted isotope separation techniques by the Nobel Prize winner Y T Lee [35] and has since been explored by many researchers [36–45].

One intermolecular bond in van der Waals molecules is known to be significantly weaker than the others. The difference in bond energies is so large that vibrational quantum energies attributed to chemical bonds between monomer molecules contained in van der Waals molecules is higher than the weak bond dissociation energy. As a result, van der Waals molecules become metastable in the case of vibrational excitation of a some monomer. If the vibrationally excited state of a monomer is coupled with the ground state through the intramolecular potential, the excited van der Waals molecule will undergo dissociation. Therefore, vibrational predissociation takes place.

This property of van der Waals molecules is of great interest in the context of the development of LEM MLIS. For example, the binding (dissociation) energy E_b of van der Waals molecules composed of polyatomic molecules lies in a range of $0.1 \leqslant E_b \leqslant 0.5$ eV, while the dissociation energy of van der Waals molecules composed of a polyatomic molecule and a noble gas atom is $E_b \leqslant 0.1$ eV [46–49]. Thus, absorption by a molecule of one or more quanta of IR radiation with a wavelength of ~ 10 μm, e.g., CO_2-laser radiation, results in the dissociation of its weak bond.

IR vibrational predissociation of van der Waals molecular clusters exemplified by $(N_2O)_2$ dimers was first reported in Ref. [50], where they were excited near the ν_3 vibrational mode of an N_2O molecule by radiation from a tunable diode laser. Photodissociation of van der Waals C_2H_4 complexes with He, Ar, Kr, C_2H_4, C_2F_4, and bigger molecular complexes was studied in Refs [37, 38] upon their excitation by a continuous CO_2 laser near the ν_7 vibrational mode of a C_2H_4 molecule. It was shown that the width and the shape of predissociation spectrum bands are consistent with the uniform broadening mechanism due to molecular dissociation. Predissociation times corresponding to the spectra of the ethylene complexes studied lie in a range from 0.3 to 1 ps. The possibility of isotope-selective dissociation of clusters by IR radiation was reported in Refs [35–39]. Many later studies were devoted to the spectroscopy and dynamics of weakly bound van der Waals molecular complexes [51–59] (see also reviews [46-49] and references cited therein).

Spectroscopic studies of modest van der Waals molecular complexes [46–49] revealed that the absorption spectra of certain dimers and small clusters (either homogeneous or heterogeneous) can be far narrower than those of unclustered molecules and look like narrow bands localized near the vibrational frequencies of monomer molecules incorporated into the clusters. This makes it possible to selectively excite and dissociate clusters (usually dimers) containing the

selected isotopomers and thereby separate isotopes. In this method, the cluster dissociation is accompanied by the escape of fragments (monomers) from the beam due to recoil processes. Thus, target molecules (dissociation products) propagate in the laboratory reference frame within a relatively large solid angle determined by the molecule mass and velocity, whereas nontarget molecules remain in the near-axial region of the cluster beam. A detection of a molecular/cluster beam by a mass spectrometer or pyroelectric detector reveals its depletion of excitable (target) molecules.

3.2 Some results

Let us consider certain results [35, 39–45] concerning the isotope-selective dissociation of van der Waals molecules in the context of their application for laser-assisted isotope separation. This method was patented [35] as a new isotope separation technique for various chemical elements by means of photodissociation of van der Waals complexes caused by the vibrational excitation of their constituent molecules.

Reference [39] reports on the selective IR photodissociation of van der Waals $Ar-BCl_3$ molecules in a molecular beam using a tunable continuous CO_2 laser. A quadrupole mass spectrometer was employed to detect and identify the molecular beam composition. The $Ar-BCl_3$ clusters were produced by supersonic expansion of a gaseous Ar and BCl_3 mixture containing a large amount of He as it passed through a continuous nozzle 50 μm in diameter [39]. To avoid the formation of $(BCl_3)_2$ dimers or larger-sized clusters, the concentration of BCl_3 molecules in the mixture above the nozzle did not exceed 1%. Uniform irradiation of the beam was achieved using CO_2-laser radiation with a power density up to 10 W cm^{-2} directed without focusing opposite to the molecular beam through the mass spectrometer ionizer. The laser beam was modulated by a chopper, and the intensity of the selected ion peak in the molecular beam mass spectrum was measured by a two-channel integrator, both under laser irradiation and without it. Ion peak intensity variations caused by the dissociation of van der Waals $Ar-BCl_3$ molecules were measured with reference to laser power and wavelength. The $Ar-BCl_3$ photodissociation spectra thus obtained are presented in Fig. 2. It demonstrates the predominance of uniform broadening and predissociation time falling in a range of 1–3 ps. Possibilities of practically applying the isotope separation method being considered were discussed in terms of effectiveness and selectivity of the process.

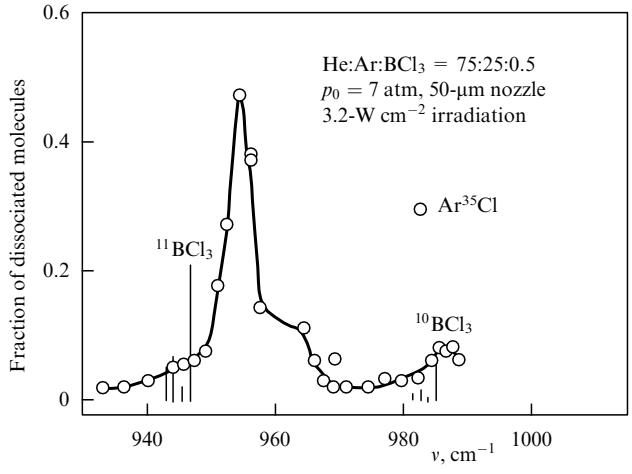

Figure 2. $Ar-BCl_3$ IR photodissociation spectrum. $Ar-BCl_3$ dimers were detected as $Ar^{35}Cl^+$ ions. The line spectrum originates from absorption of BCl_3 molecules dissolved in solid argon at 75.8 K. BCl_3 absorption linewidths in the matrix are less than 0.1 cm^{-1} [39].

IR vibrational predissociation of van der Waals molecules was studied from the standpoint of its application to isotope separation using $(SF_6)_M Ar_N$ complexes (where $1 \leqslant M \leqslant 3$, $1 \leqslant N \leqslant 9$) [40–43]. These complexes formed in a free jet during expansion of the SF_6 mixture with argon under an SF_6 partial pressure of 0.5%, as it passed through a 0.1-mm nozzle. Predissociation was found to be an isotope-selective process. When a natural mixture of SF_6 isotopomers diluted by argon gas was irradiated with continuous 20-W CO_2 laser [40, 43], $^i SF_6$ enrichment coefficients ($i = 32, 34$) were higher than $K_{enr} \approx 1.2$ (Fig. 3) [40]. The dependence of enrichment coefficients on the frequency of exciting laser radiation was elucidated. The enrichment coefficient was defined in Refs [40, 43] as

$$K_{enr} = \frac{X_E(1 - X_D)}{X_D(1 - X_E)}, \tag{3.1}$$

where X_E and X_D are the mean molar fractions of the enriched and depleted target isotope components ($^{34}SF_6$ in the

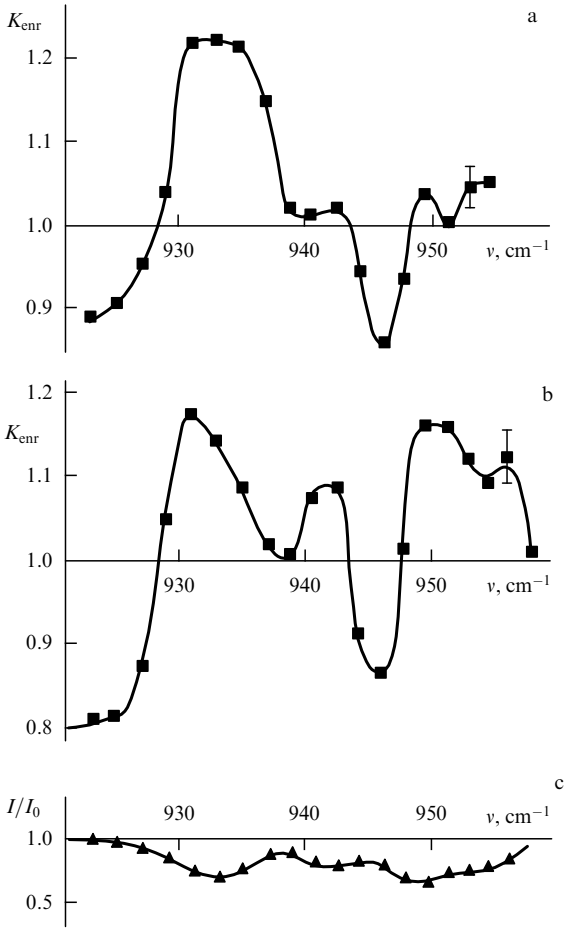

Figure 3. Dependence of the relative enrichment coefficient K_{enr} measured in a molecular beam on frequency ν of exciting laser IR radiation at an above-nozzle temperature and pressure (a) $T_0 = 237$ K, $p_0 = 1.5$ atm, and (b) $T_0 = 225$ K, $p_0 = 1.4$ atm, respectively. SF_6 partial pressure in Ar is 0.5%. (c) Relative weakening of beam intensity, I/I_0, measured from the mass peak of $^{32}SF_5^+$ depending on laser frequency; experimental conditions are the same as indicated in figure b [40].

experiment being described), respectively. It was shown that the proper choice of the wavelength of exciting laser radiation makes it possible to obtain a beam either enriched with or depleted of the selected isotopomer. It was revealed that at certain laser IR radiation wavelengths, nonselective cluster dissociation occurs. The authors of Refs [40, 43] maintain that this finding can be used to optimize isotope separation by suppressing clusterization (see Section 4).

Let us recall that the effective separation of isotopes by IR vibrational predissociation of van der Waals clusters in a free jet is possible under conditions ensuring the presence of a relatively large fraction of clusters in the beam. In principle, such conditions can be realized by maintaining high gas pressure p_0 and low temperature T_0 above the nozzle. However, the larger the fraction of clusters (in this case of $(SF_6)_M Ar_N$) clusters) contained in the beam, the broader their size distribution. All these clusters have different IR absorption spectra [40, 46, 47, 51–54], which accounts for a very complicated dependence of isotope enrichment on the laser radiation wavelength, because $(^i SF_6)_M Ar_N$ clusters of different sizes can dissociate at each selected wavelength, which contributes to the enrichment and/or depletion of a given isotopomer.

Reference [44] demonstrated the possibility of UF_6 cluster dissociation under the effect of IR radiation. These experiments were carried out with a view to 'purify' a molecular beam of clusters during realization of the MLIS method based on IR MPD in a gas-dynamically cooled molecular flow. The possibility of applying IR vibrational predissociation of van der Waals clusters for uranium isotope separation was considered in Ref. [45].

Thus, the results of research show that the IR vibrational predissociation technique for van der Waals molecules allows isotopes to be separated in gas-dynamically cooled jets and flows.

In the context of practical application of this method for isotope separation, it is worth mentioning its relatively low efficiency due to certain intrinsic features, such as the low throughput. The assessment made in Ref. [39] indicates that though one can remove about 70% of the $Ar-{}^{10}BCl_3$ molecules from a beam, this is only a small fraction of total ${}^{10}BCl_3$ molecules contained in the beam. The concentration of van der Waals dimers in the beam is but a few percent of the total BCl_3 concentration above the nozzle. Therefore, the separation of 1 mole of ${}^{10}BCl_3$ from a natural isotopomer mixture in the experimental setup described in preceding paragraphs (nozzle with diameter 50 μm, total gas pressure above nozzle of about 7 atm) would require continuous irradiation, gas recirculation, and collection of the products over several years. However, the capacity of such a facility can be increased by as much as 100 times by using higher-power vacuum pumps and nozzles with larger-diameter orifices. It will permit reducing the total duration of the procedure to a few days [39].

4. Selective control of molecule clusterization in jets and flows

4.1 Basis of the method

A fairly well-studied method for selective control of molecule clustering in jets and flows with the use of IR lasers is presently regarded as one of the feasible and most promising techniques for laser isotope separation [11, 42, 43, 45, 60–63]. The method is based on selective vibrational excitation of molecules of a given isotope composition immediately after the exit of the gas-dynamically cooled gas from the nozzle due to its expansion, which hampers or prevents subsequent molecule clusterization. To effectively realize such a process and ensure its high selectivity, the precise balance between the rates of jet gas-dynamic cooling necessary for evolving clusterization and selective excitation of molecules with a given isotope composition needs to be maintained in order to suppress their clusterization.

The necessary conditions of controllable clusterization can be provided by choosing a nozzle with a proper orifice design, diameter, and operating mode (pulsed or continuous) and gas composition, temperature (T_0), and pressure (p_0) above the nozzle. Moreover, spatial localization of the irradiated site and IR radiation characteristics (wavelength and intensity) are of primary importance. All these conditions for a concrete object should be chosen on an individual basis.

It is worthwhile to note that the physical nature of the processes being observed varies in such experiments depending on the location of the irradiated area with respect to the nozzle cut. Excitation of molecules near the nozzle cut results in the suppression of subsequent clustering and attenuation of the observed cluster signal. If molecules are excited far from the nozzle cut, cluster dissociation prevails (see Section 3), and the cluster signal decreases under the effect of IR vibrational predissociation proper. Transition from one process to the other is the main factor determining the behavior of the measured cluster signal (see Section 4.2).

An important aspect of the method under consideration concerns with achieving the high degree of product selectivity (or high enrichment coefficients), when taking into account the relatively fast exchange of vibrational energy between selectively excited and unexcited molecules in the excitation zone due to a relatively high pressure near the nozzle. To reduce or prevent the rapid energy transfer between isotopomers under experimental conditions, a highly diluted gas mixture containing less than approximately 0.5–1% of molecules in the carrier inert gas is usually used. Both increased dilution of molecules in the inert gas and decreased total gas pressure above the nozzle contribute to improving isotope selectivity of the process.

4.2 Results of research

The first experimental data demonstrating the possibility of using lasers to effectively suppress dimer formation in supersonic free jets were obtained by the group headed by H van der Bergh of the École polytechnique fédérale de Lausanne EPFL [64–66]. The researchers studied suppression of clusterization of argon-diluted SF_6 molecules by irradiating the mixture with a 24-W continuous wave (cw) laser at the exit from the supersonic nozzle with an opening diameter of 100 μm [65, 66]. A skimmer 1 mm in diameter placed 13 mm from the nozzle was used to split the molecular beam from the jet. The gas temperature above the nozzle was varied from 150 to 600 K either by cooling the source in liquid-nitrogen vapor or by resistive heating of the source; this allowed cluster content to be controlled in the beam. The beam detector was a quadrupole mass spectrometer. The laser beam was directed normally to the molecular beam. Laser radiation was focused onto the gas expansion zone with a KCl lens having a focal length of 30 cm and the spot diameter at the lens focus (in the irradiated area) of 0.5 mm. Sometimes, a lens with a focal length of 20 cm was utilized; in such cases, the

spot had a diameter of 0.3 mm. The ion signal from $(SF_6)_2$ dimers in the irradiated gas was measured taking account of the laser power and the distance between the exit point from the nozzle and the irradiated area.

It was revealed that $(SF_6)_2$ cluster formation was strongly suppressed by SF_6 monomer irradiation in the collisional region at the exit from the nozzle by resonance laser radiation with a power of several kilowatts (Fig. 4). Vibrational predissociation of clusters originated, in parallel with the suppression of clustering, as the distance between the nozzle and irradiated area increased. Therefore, the cluster signal was attributable to both these processes. At large distances from the nozzle, attenuation of the cluster signal was largely due to vibrational predissociation of the clusters (see Section 3). It was shown in Refs [65, 66] that the laser-induced signal strongly depends on the exciting radiation wavelength, the distance between the nozzle and the irradiated area, and the parameters of the gas above the nozzle because of IR absorption by clusters in the beam. The authors of Refs [65, 66] observed the suppression of the cluster formation upon excitation of both $^{32}SF_6$ and $^{34}SF_6$ molecules (Figs 4a and 4b, respectively).

The isotope-selective control of molecule clusterization by an IR laser and its application for isotope separation was demonstrated for the first time in Refs [60, 61]. Experiments were carried out with SF_6 molecules with a natural isotope composition (^{32}S — 95 %, ^{33}S — 0.76 %, ^{34}S — 4.22%) strongly diluted in argon (at pressure ratios of 1:100 or 1:200). Such a strong dilution of SF_6 in argon increases the effectiveness of gas-dynamic cooling of the molecules, promotes clustering and the formation of mixed SF_6Ar_M clusters, and interferes with energy exchange between molecules of different isotope compositions. The gas temperature and pressure above the nozzle were $T_0 = 233$ K and $p_0 = 1.5$ atm, respectively. The gas-dynamic jet was produced in a nozzle 0.1 mm in diameter. The molecular beam was extracted from the jet with the aid of a skimmer 1 mm in diameter placed 10 mm away from the nozzle. Molecules were selectively excited in the gas-dynamic expansion zone at the exit from the nozzle by focused radiation from a 20-W continuous wave CO_2 laser with a tunable generation wavelength. The laser beam was directed perpendicular to the jet axis.

It was demonstrated that selective excitation of $^iSF_6$ isotopomers ($i = 32$, 33, 34) in the gas expansion zone (0.2 mm from the nozzle cut) significantly decreases the concentration of $^iSF_6Ar_M$ clusters in the beam (Fig. 5). It is believed that the $^iSF_5Ar^+$ ion signal reflects in the first approximation the concentration of $^iSF_6Ar$ clusters in the beam. Enrichment coefficients were $K_{enr} \approx 2$. Reference [60] gives evidence that the enrichment coefficient strongly depends on the degree of SF_6 dilution with argon: the lower the concentration of SF_6, the higher the enrichment coefficient due to a decrease in the vibrational–vibrational energy exchange rate between molecules. As was shown in Ref. [60], a rise in the SF_6 partial pressure in argon from 0.5 to 3% leads to a decrease in the enrichment coefficient from roughly 2 to 1. This method enabled the authors of paper [60] to separate silicon isotopes in SiF_4 molecules, and bromine isotopes in CF_3Br.

SF_6 molecules in Ref. [42] and SiF_4 and CF_3Br molecules in Refs [43, 62] were employed in studying the separation of sulfur, silicon, and bromine isotopes, respectively, by a combination of two processes, suppression of molecule clusterization and vibrational cluster predissociation, exploiting two frequency-tunable CO_2 lasers. The isotope-selective suppression of clustering was confined to the gas expansion zone at the exit from the nozzle, while selective cluster dissociation went on in the cluster free-flight zone of the

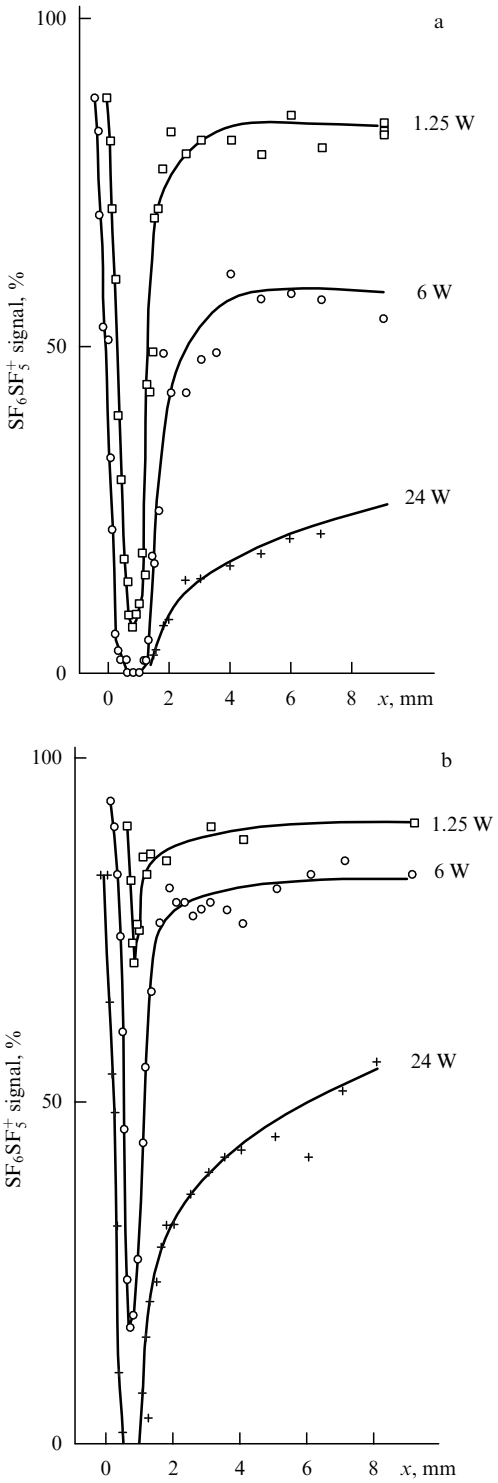

Figure 4. Measured depletion of the $SF_6SF_5^+$ ion signal as a function of distance x between the irradiated area and the nozzle during irradiation of (a) $^{32}SF_6$ monomers at the wavelength $\lambda = 10.551$ μm (10P(16) line), and (b) $^{34}SF_6$ monomers at the wavelength $\lambda = 10.741$ μm (10P(34) line) in the jet collisional region by a 1.25-, 6-, or 24-W laser. Gas pressure and temperature above the nozzle are $p_0 = 1.7$ atm and $T_0 = 222$ K, respectively [66].

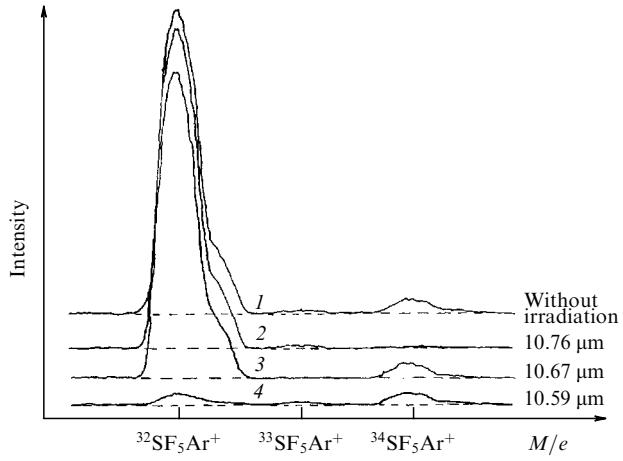

Figure 5. Isotope-selective condensation of 0.5% SF_6 in argon in the absence of irradiation (curve *1*); $^{34}SF_6$ irradiation at a laser wavelength of 10.76 μm, 10P(36) line (curve *2*); $^{33}SF_6$ irradiation at a laser wavelength of 10.67 μm, 10P(28) line (curve *3*); $^{32}SF_6$ irradiation at a laser wavelength of 10.59 μm, 10P(20) line (curve *4*). M/e — mass number. $T_0 = 225$ K and $p_0 = 1.5$ atm are above-nozzle gas temperature and pressure, respectively. Laser power density is about 20 kW cm^{-2}. Irradiation of a given isotopomer clearly and selectivity suppresses SF_6Ar cluster formation for a vibrationally excited isotopomer [60].

molecular beam. In experiments on selective suppression of $^{32}SF_6$ clusterization, for example, the beam of SF_6 molecules contained unclustered $^{32}SF_6$ molecules and $(^{34}SF_6)_M Ar_N$ clusters. The second laser was then put on to cause selective vibrational predissociation of $(^{34}SF_6)_M Ar_N$ clusters. Recoil of $^{34}SF_6$ molecules resulted in their ejection from the near-axial beam region and thereby promoted its further enrichment with $^{32}SF_6$ isotopomers. The joint action of two lasers resulted in an increase in enrichment coefficients up to $K_{enr} \geqslant 2.1$ [43].

Reference [63] describes a model of the above process and the main relations for calculating enrichment and depletion coefficients for laser-induced QF_6 excitation (where $Q = S$, U) in overcooled supersonic expanding flows and in flows containing a carrier gas (argon or another) that passes through a tube with cold walls at a subsonic speed. The authors consider situations in which the laser beam is oriented either parallel or perpendicular to the flow direction. Isotope-selective excitation of $^iQF_6$ molecules interferes with their condensation during cluster formation and with their condensation on the tube walls, resulting in the enrichment of the passing gas with the target (excited) isotopomer and isotopic depletion of the clusters deposited on the walls. The experimentally examined changes in the ratios for $^{32}SF_6/^{34}SF_6$ ($K_{enr} \approx 2.10$) [43] and $^{235}UF_6/^{238}UF_6$ ($K_{enr} \approx 1.02$) [33] (see Section 2) are consistent with the computed ones. The suggested model [63] has recently been revised in Ref. [67] to develop a new statistical model for boron isotope separation by suppressing cluster condensation.

The potential of the method considered in this section for selective laser control of molecule clusterization in gas-dynamically expanding jets and flows is briefly discussed in Refs [11, 45] in the context of uranium isotope separation, e.g., by the SILEX technique (see Section 9). Eerkens and Kim [11] compared this approach with other methods of molecular laser isotope separation.

5. Isotope separation involving the capture of low-energy electrons by molecules

5.1 Processes behind the method

One of the alternative low-energy methods for molecular laser isotope separation is that based on the capture of low-energy electrons by molecules [68]. Electron–molecule interactions result in both elastic and inelastic collisions. The probability of inelastic collisions leading to dissociative and nondissociative attachments of electrons to molecules is large at low electron energies (0–15 eV) [69, 71]. In the case of dissociative attachment, a molecule dissociates, giving rise to a negatively charged constituent, namely

$$e + XY \rightarrow X^- + Y. \tag{5.1}$$

Upon nondissociative electron attachment, an excited negative molecular ion XY^{-*} is the first to form. Thereafter, it can be neutralized as a result of electron autodetachment. However, the negative molecular ion may long remain in a quasistationary excited state; it stabilizes with time due to intramolecular relaxation, collisions with the surrounding gas, or spontaneous emission [72, 73].

Total cross sections of low-energy electron capture by molecules are characterized by large values [69–71,74]. The total capture cross section of electrons with an energy of $10^{-4}-10^{-1}$ eV by an SF_6 molecule at room temperature is roughly 10^{-12} to 10^{-14} cm^{-2}; it lessens as electron energy increases [69]. Cross sections of dissociative electron attachment to molecules are much smaller. In the above electron energy range, cross sections for SF_5^- ion formation via the reaction channel

$$e + SF_6 \rightarrow SF_5^- + F \tag{5.2}$$

are roughly two orders of magnitude smaller than for the mother SF_6^- ion formation [69]. All the same, these are rather high values.

Negative mother SF_6^- ions largely form at a zero or close-to-zero electron energy. Collisionally stabilized SF_6^- ions have (at 300–500 K) longer lifetimes relative to the characteristic autodetachment time. Time-of-flight measurements [75–77] showed that in the absence of collisions the lifetime is more than 1 μs (between 10 and 68 μs) (see Ref. [69] and references cited therein). Similar measurements by the ion cyclotron resonance technique revealed that the lifetime of SF_6^{-*} is actually much longer (a few milliseconds) [78, 79]. As shown in Refs [77, 80], the difference can be attributed to the fact that the lifetime of many long-lived negative polyatomic ions strongly depends on experimental conditions (electron kinetic energy, molecular internal energy and its distribution over degrees of freedom, and gas temperature).

The attachment of low-energy electrons to molecules at room temperature largely gives rise to long-lived mother SF_6^- anions with the formation of only small amounts (a few percent) of SF_5^- anions via reaction $SF_5^- + F$ due to dissociative attachment of electrons [69]. SF_6^- anion forms at electron energies lying within a very narrow (resonance) region near zero energy (lower than ≈ 0.3 eV) with the largest known electron capture cross section of about 10^{-12} cm^2. The SF_5^- anion forms (depending on experimental conditions) when electrons with higher energies (up to about 0.3–0.5 eV) are captured [69].

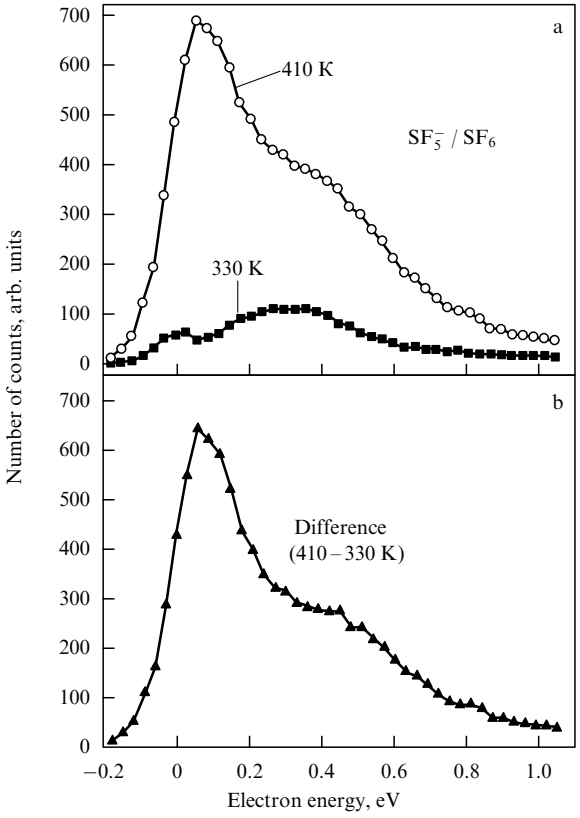

Figure 6. Dissociative electron attachment to SF_6 molecules resulting in the formation of SF_5^- anions: (a) at two different temperatures of molecules in the beam (all other conditions being equal), and (b) difference spectrum [84].

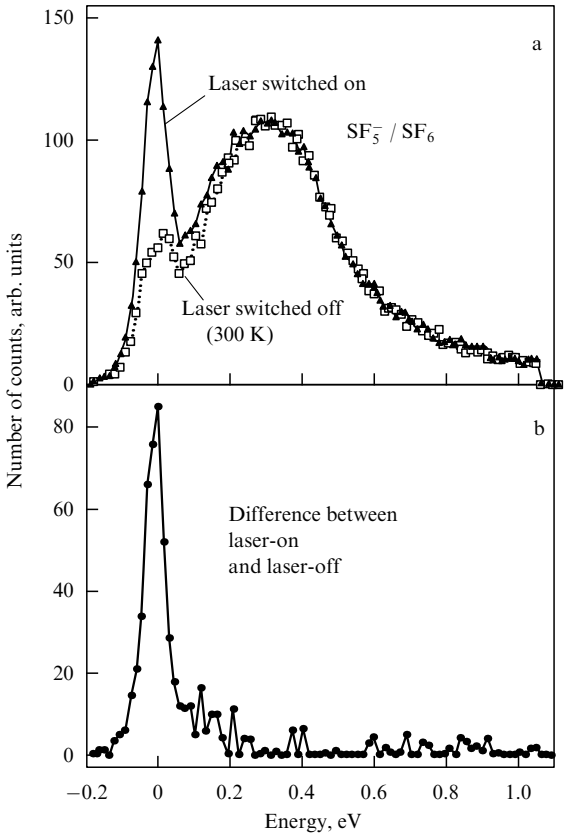

Figure 7. Dissociative electron attachment to SF_6 molecules at 330 K giving rise to SF_5^- anions: (a) with laser irradiation of SF_6 at 10P(28) line (936.8 cm^{-1}) and without it, and (b) difference spectrum [84].

Certain authors [81–84] demonstrated that thermal heating of SF_6 molecules is accompanied by an enhanced yield of SF_5^- anions and the appearance of a threshold peak (near the zero electron energy) that becomes predominant at high (above 400 K) temperatures (Fig. 6). A rise in the yield of negatively charged fragments with increasing temperature was also observed in experiments with other molecules [85–89]. The authors of Refs [83, 90] studied the endothermicity of the dissociative electron attachment to an SF_6 molecule with the formation of an SF_5^- anion. Also, it was shown in Ref. [84] that the yield of SF_5^- ions via reaction channel (5.2) increases appreciably if the excitation of the ν_3 vibrational mode of SF_6 molecules by resonant radiation of a continuous wave CO_2 laser precedes collisions with electrons (Fig. 7).

5.2 Principles of the method and certain results

Let us consider the principles underlying the method of interest for separating isotopes as exemplified by a natural mixture of isotopomers, e.g., $^{34}SF_6/^{32}SF_6$ or $^{235}UF_6/^{238}UF_6$. In this method, molecules containing target isotopes ($^{34}SF_6$ or $^{235}UF_6$) are selectively excited in a mixture of isotopomers in a molecular flow or jet by IR laser radiation. Then, the molecules are allowed to collide with low-energy electrons. Dissociative attachment of the low-energy electrons to the molecules gives rise to the formation of stable negatively charged fragments ($^{34}SF_5^-$ or $^{235}UF_5^-$). To obtain a negatively charged fragment, the energy of the attached electron must be at least equal to the energy necessary for molecule dissociation minus the excitation energy and the energy of an electron affinity to the resulting fragment to which the electron attaches [68]. (Electron affinity to the fragment is the electron–fragment binding energy.)

It was shown in Section 5.1 that the vibrational excitation of molecules results in a significant increase in the effective cross section of dissociative electron attachment (Fig. 7), i.e., in the enhancement of the probability of dissociation of excited molecules compared with unexcited ones, and leads to the formation of negatively charged fragments ($^{34}SF_5^-$, $^{235}UF_5^-$) via reaction channel (5.2). It is this process that underlies the isotope separation method of interest. The resultant ions containing a target isotope and the neutral molecules are separated either by applying electric fields or in chemical reactions [68].

The formation of negatively charged ions in the above process considerably simplifies the separation of a target isotope from the remaining mixture of neutral molecules and facilitates effective enrichment of the target isotope. To recall, sources of low-energy monochromatic electrons (electron guns) are needed to realize the method under consideration. Such sources can be, for example, spectrometers of passing electrons with a trochoidal monochromator allowing electrons with a narrow energy distribution (of width $\leqslant 30$ meV) rearrangeable within a wide energy region to be obtained [91, 92]. The principle of action of a trochoidal monochromator consists in the passage of an electron beam through crossed electric and magnetic fields. It induces spatial electron velocity dispersion. Perforated lenses make it possible to cut out a portion of the dispersed beam to obtain a quasimonochromatic electron beam [91, 92].

The application of the method described in this section for isotope separation was proposed (patented) by Chen and Chantry [68], where SF_6 and UF_6 molecules were utilized as model objects. No data on process selectivity, enrichment coefficient and efficiency are presented in Ref. [68]. We are unaware of the declassified publications dealing with the use of this method for isotope separation. At the same time, results of research demonstrating a significant enlargement of the cross sections of dissociative electron attachment to vibrationally [84] and thermally [84–88] excited molecules give grounds to conclude that the method in question can be employed to separate isotopes.

It should be noted, however, that the method remains to be studied more thoroughly. Its efficiency appears to be low because cross sections of dissociative electron attachment to molecules are much smaller (by roughly two orders of magnitude) than those of electron capture with the formation of negatively charged ions. Moreover, the practical realization of the method encounters difficulties. Further studies are needed to optimize the parameters of the isotope separation process using up the method in question.

6. Selection of molecules embedded in nanodroplets (clusters) of superfluid helium

6.1 General remarks

A method for the selection of molecules inserted into nanodroplets (clusters) of superfluid helium was described in Refs [93–96]. The principles of the method and certain results obtained with it are discussed below (see also review [97]), with special reference to laser-assisted separation of isotopes of elements with medium and large masses, such as Si, U, W, and Os. Isotope shifts in IR absorption spectra of molecules containing these elements are relatively small ($\Delta\nu_{is} \leqslant 5-10$ cm^{-1} for silicon-containing molecules, and $\Delta\nu_{is} \leqslant 1$ cm^{-1} for UF_6, WF_6, OsO_4). As a result, the linear and multiphoton absorption spectra of molecules containing different isotopes either strongly or almost completely overlap not only at room temperature but also in gas-dynamically cooled jets and flows. Therefore, selective excitation of molecules becomes extremely difficult. A different situation takes place when superfluid helium clusters are used. Their low temperature ($T \leqslant 0.4$ K) accounts for the very narrow IR absorption spectra of molecules contained in them. Such sharp narrowing of IR absorption spectra of molecules inserted into helium droplets is an important advantage for their selective excitation and laser separation of isotopes.

6.2 Physical foundation of the method

It was shown both in experiments [98–101] and theory [102–104] that helium-4 nanodroplets (clusters) with $N \geqslant 50-100$ particles are superfluid [105]. The molecules imbedded in them are free to rotate and have very narrow IR absorption spectra due to the rather low temperature of the nanodroplets ($T \approx 0.37$ K) [98, 99, 106–112]. For example, the total absorption bandwidth of $^{32}SF_6$ vibrational mode ν_3 in a superfluid helium nanodroplet is only 0.25 cm^{-1} [113–115]. In this case, the IR absorption spectra are virtually totally 'separated' not only in molecules showing relatively large ($\geqslant 5-10$ cm^{-1}) isotope shifts, e.g., SF_6, SiF_4, but also in those containing heavy elements. This provides an opportunity for highly selective excitation of only those helium clusters in the beam that contain molecules of the desired isotope composition.

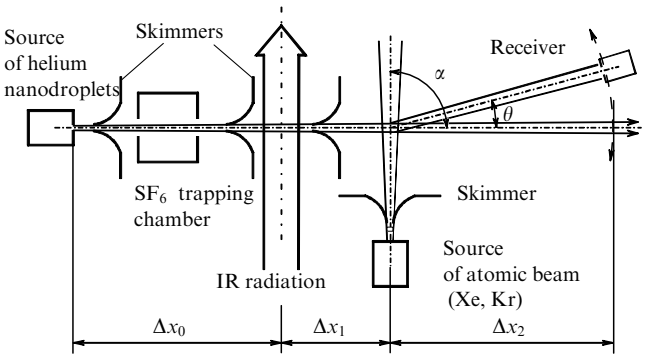

Figure 8. Schematic of an experiment on molecule selection inside helium nanodroplets [94, 95].

Radiation absorption by molecules inserted into a helium droplet causes heating and evaporation of a certain number of atoms [98, 99, 106–111, 115]. For example, absorption of a single quantum of CO_2-laser radiation ($\lambda \approx 10$ μm, $\hbar\omega \approx 0.12$ eV) causes evaporation of roughly 200 atoms from a helium nanodroplet [98, 107, 111, 115]. Evaporation results in a decrease of droplet temperature which stabilizes again at $T \approx 0.37$ K [98, 109, 111, 116]. Both heating and evaporation of atoms occur immediately after photon absorption (within $\leqslant 10^{-8}-10^{-9}$ s) [115–118]. All these factors can be used for molecule selection in superfluid helium nanodroplets in terms of isotope and component compositions.

The method is as follows (Fig. 8) [94, 95]. A beam of superfluid helium nanodroplets (clusters) with imbedded molecules is subjected, at distance Δx_0 from the nozzle, to intense IR laser radiation in resonance with vibrations of the molecules with a given isotope composition. Only those helium clusters in the beam undergo excitation that contain resonantly excited molecules. The absorbed energy heats nanodroplets and evaporates helium atoms. The atoms being evaporated isotropically escape from the cluster.

In large clusters ($N \geqslant 10^6-10^7$ atoms), the atomic binding energy is roughly equal to that in bulk liquid helium (≈ 7.2 K [119]) but drops as the cluster size decreases. When an excited cluster absorbs 5–10 quanta from the laser radiation field with a wavelength of roughly 10 μm, it becomes 1000–2000 atoms smaller. If a molecule-doped helium cluster in the beam contains about $(2-3)\times 10^3$ atoms, absorption of IR photons is accompanied by an appreciable decrease in its size. Given that a cluster contains fewer than 10^3 atoms, its laser radiation excitation may result in complete fragmentation with the formation of free (totally 'naked') SF_6 molecules. In other words, IR excitation will lead to a marked alteration of cluster size distribution inside the beam compared with the distribution in the starting beam. In this case, the size of selectively excited clusters will be much smaller than that of unexcited ones.

The next step consists in size-specific selection of the clusters [93–96]. To this end, the authors took advantage of scattering of the cluster beam from a secondary molecular (or atomic) beam [120–122] intersecting it after laser excitation at the distance $\Delta x_0 + \Delta x_1$ from the nozzle (Fig. 8). The scattering beam may be a beam of xenon or krypton atoms. Scattering from the secondary beam leads to angular disintegration of the cluster beam [121, 122]. Helium cluster

scattering from the secondary beam is characterized by trapping of beam particles by nanodroplets [120–122]. The particle's momentum is transferred to the nanodroplet. It gets heated and its atoms evaporate (as under the effect of laser excitation), the number of evaporated atoms being determined by the energy of the captured particle. Around 100–200 atoms are evaporated from a cluster produced from a monoatomic gas, and over 600 atoms from a cluster produced from polyatomic molecules, such as SF_6 [121]. Smaller-sized helium clusters scattered from the intersecting beam are deflected at larger angles. Thus, selective excitation of molecules inside helium clusters by intense laser radiation and subsequent deflection of different-sized clusters at different angles can be employed to select molecules imbedded in helium nanodroplets.

6.3 Some results

References [94, 95] report on an analysis of the possibility of applying the above method for isotope separation, as exemplified by SF_6 molecules resided inside superfluid helium clusters. The xenon gas beam was considered as an atomic beam scattering helium clusters. These numerical simulations revealed the optimal (in terms of laser radiation frequency and intensity) conditions necessary for the selective excitation of molecules inside the clusters, with reference to the factors influencing the efficiency and selectivity of isotope separation. Such factors include the nonselective evaporation of helium atoms during trapping of molecules by superfluid droplets (Fig. 9), the Poisson distribution of molecules inside nanodroplets upon their trapping, the finite width of the atomic velocity distribution in the scattering beam, the presence of double atom–cluster collisions, and the finite extension of the region of interaction between the cluster beam and the scattering atomic beam (see Fig. 8).

It was shown that the main factor responsible for impaired selectivity of the isotope separation process is nonselective thermal evaporation of helium atoms from the clusters associated with the trapping of high-energy molecules (see Fig. 9); hence, the necessity to cool down the gas in the trapping chamber in the case of large molecules, such as SF_6, OsO_4, and UF_6. For example, the capture of an SF_6 molecule at 150 K results in the evaporation of no more than 160–170 atoms per cluster. As follows from Fig. 9, in this case the integral selectivity at angles $\theta \geqslant 0.04$ rad is roughly ten times that at room temperature.

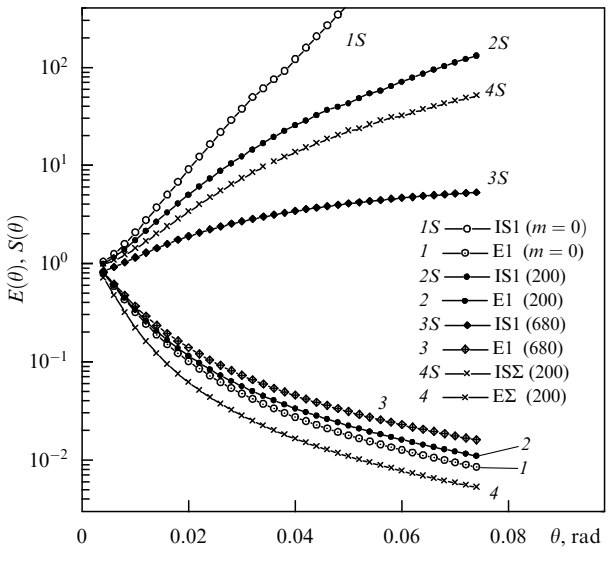

Figure 9. Angular dependences of effectiveness (curves *1–3*) and integral selectivity, i.e., averaged selectivity for clusters propagating outside the angle θ (curves *1S–3S*), for different numbers m of helium atoms evaporating during molecule trapping ($m = 0$, 200, and 680). Curves *4* and *4S* are the angular dependences of effectiveness and selectivity, respectively, for a cluster beam containing singly and doubly doped clusters (in thee ratio 2:1, $m = 200$) [95].

Reference [95] also reports an estimation of the yield of enriched products based on real parameters of helium cluster beams and of the performance of diffusion pumps exploited in these experiments [107, 111]. It turned out that molecule excitation in a continuous cluster beam by a pulsed CO_2 laser operated at the frequency repetition rate $f \approx 500$ Hz yields enriched SF_6 at a rate of 10^{13} molecules per second or 3.6×10^{16} molecules per hour (an equivalent to roughly 0.01 mg h^{-1}) with the integral selectivity IS ≈ 10. Of course, this is a very low throughput even making allowance for the fact that the estimates were obtained only for a concrete small unit employing a single diffusion pump.

6.4 Comparison with infrared multiphoton dissociation of molecules

The comparison of the method under consideration with that built around an infrared multiphoton dissociation of UF_6 molecules [7, 123] in a gas-dynamically cooled flow was undertaken in Ref. [95] taking account of the known experimental parameters. It demonstrated that the IR MPD of molecules with selectivity $S \approx 3-5$ yields enriched products at a rate of 10^{15} molecules per second or 3.6×10^{18} molecules per hour, i.e., roughly two orders of magnitude higher than with the use of helium nanodroplets.

It should be recalled that a high selectivity of dissociation in IR MPD of molecules with a small isotope shift is attainable only in multifrequency IR fields, which considerably complicates isotope separation process. Moreover, high energy densities and a significantly greater (more than two orders of magnitude) contribution of laser photons to molecule dissociation have to be realized due to a pronounced energy dissociation and poor selectivity of the process in which a large fraction of laser photons are utilized to excite molecules containing a nontarget isotope.

One of the advantages of the method considered in this section for selective excitation and dissociation of clusters with target molecules is that it requires only single-frequency radiation of a moderate-power laser. This means that one laser can be used to irradiate larger volumes than in the MPD of molecules. Moreover, it ensures a higher degree of selectivity.

Another advantage of the method is the possibility of applying microwave radiation for selective excitation of molecules inserted into nanodroplets. It was experimentally shown (see Refs [107, 111] and references cited therein) that the application of high-power microwave radiation for molecule excitation inside helium nanodroplets and their evaporation produces the same effects that are achieved with the help of IR lasers.

Other important advantages of employing superfluid helium clusters for molecule selection by the method described above are the very low binding energy of atoms ($\leqslant 7.2$ K [119]) and free rotation of molecules in the clusters. Due to the low atomic binding energy in the clusters, absorption of a single IR photon significantly reduces the

cluster size. Moreover, the binding energy further drops with decreasing the cluster size [119], which accounts for lower expenditures of pumping energy.

Unlike isotope-selective IR MPD (see, for instance, papers [7, 14, 16, 123] and references cited therein) applicable only to polyatomic molecules, the method considered in this section is suitable for the selection of small molecules, including diatomic ones. Due to free rotation, IR absorption spectra of small (e.g., di- and triatomic) molecules inside superfluid helium nanodroplets contain separated narrow vibrational–rotational lines [98, 107, 111], which enables a highly selective excitation of molecules. Then, the size distribution of helium clusters doped with small molecules is not as strongly distorted as that in the case of large molecules, making it possible to enhance the selectivity of dissociation of laser-excited molecules (Fig. 9). The main drawbacks of the method come from the technical difficulties in carrying it out and the comparatively low throughput.

Bearing in mind the above estimates and the results of a comparison of the two methods, it is currently believed that the creation of industrially relevant modules for laser separation of uranium isotopes by the IR MPD of UF_6 molecules is commercially inexpedient at the modern level of laser technologies [124]. Further studies made on existing facilities are needed to resolve problems pertinent to the development of laser systems themselves and the optimization of gas-dynamic flows. Therefore, the method for molecule selection inside helium nanodroplets can at present find application only for laser-assisted separation of exotic molecules and/or small amounts of matter.

7. Interaction between highly vibrationally excited and unexcited molecules with molecules (clusters) condensed on a cold surface

7.1 Selected remarks

Let us consider, from the standpoint of laser isotope separation, the method proposed in Refs [125–128] and the results of these studies concerning the interaction between intense beams of highly vibrationally excited molecules (SF_6, CF_3I) and molecules (clusters) condensed on a cold ($T_s \approx 80-85$ K) surface. The authors evaluated the probability of reflection of unexcited molecules and molecules that passed into high vibrational states ($E_{vib} \approx 0.3-2.0$ eV) after excitation by high-intensity IR laser radiation on a cold metallic surface coated with molecules (clusters). Also, the probability of excited and unexcited molecules passing through cooled multichannel metal plates and cones placed at an angle to the beam axis was ascertained.

The experiments revealed the dependence of the probabilities of molecule reflection from the surface and passage through multichannel plates and cones on the parameters of exciting laser radiation, the characteristics of the incident molecular beam, and the beam incidence angle. It was shown that the probability of highly vibrationally excited molecules passing through the plates and cones and of their reflection from the surface is much higher than that of unexcited molecules. These findings suggest that the method in question can be applied to separate molecules differing in isotope (component) composition.

Experiments designed to study the interaction of atoms and molecules with the solid surface (see Refs [21, 129]) yielded some important results.

First, there is, as a rule, no potential barrier for particle trapping in the case of physical atom or molecule adsorption on a cold, clear or particle-coated surface [21, 129]. Due to this, the probability of particle trapping decreases with increasing energy E_i of atoms or molecules, because trapping at high E_i occurs if a larger portion of the incident particle energy is utilized [21, 129]. In particular, trapping into the potential with the effective potential well depth ε occurs if a part of the incident particle's energy spent in collisions is greater than $E_i/(E_i + \varepsilon)$ [21].

Second, the lifetime of an atom (or molecule) adsorbed on the surface is determined by the desorption energy E_{des} and surface temperature T_s [129]:

$$\tau = \tau_0 \exp\left(\frac{E_{des}}{k_B T_s}\right), \tag{7.1}$$

where τ_0 is the pre-exponential factor, roughly of the same order of magnitude as the particle's vibration period ($\tau_0 \sim 10^{-13}-10^{-11}$ s), and k_B is the Boltzmann constant. Finally, the probability of molecule desorption from the surface, P_{des}, depends on the molecule–surface binding energy E_b and surface temperature T_s [21, 129]:

$$P_{des} \sim \exp\left(-\frac{E_b}{k_B T_s}\right). \tag{7.2}$$

In the absence of a potential barrier for molecular adsorption, the binding and desorption energies are equal: $E_b = E_{des}$ [129].

In the case of a molecule-coated surface, E_b is the molecule binding energy on the surface or inside the clusters. Therefore, if the total energy of a molecule in a beam incident on a cold surface overlaid with molecular (cluster) layers is lower than the molecular binding energy in the clusters and the molecule–surface binding energy, the molecules will be trapped by the interaction potential and remain on the surface. If the total molecular energy exceeds the above values, a molecule may be reflected from the surface. However, this is only a simplified model. Due to rapid relaxation during molecule–surface interaction [129–131], all or part of the molecular energy can be lost or redistributed between different degrees of freedom. This is likely to make the potential barrier insurmountable, and the molecules end up trapped on the surface.

The higher the molecular energy, the more time needed for its complete relaxation [21, 130, 131]. Therefore, the coefficient of molecule reflection from the surface (or fraction of reflected molecules) is a function of the molecular energy and also depends on its distribution between different degrees of freedom [21, 132]. Due to multiphoton IR absorption [7, 14, 128], a relatively high energy (comparable with the dissociation energy of molecules) can be put into vibrational degrees of freedom. Therefore, it can be assumed that the probability of reflection of highly vibrationally excited molecules from the molecular (cluster) layers condensed on the surface is significantly higher than the probability of reflection of vibrationally cold (unexcited) molecules. This assumption was confirmed in experiments [125, 126], where SF_6 and CF_3I molecules were passed through a cold multichannel plate, and experiments [127], in which CF_3I molecules passed through a cooled cone. The layout, methods, and results of these experiments are described in Sections 7.2 and 7.3.

7.2 Experiment and research method

The essence of the method is illustrated in Fig. 10. An intense (over 10^{20} molecules per sr per s) wide-aperture (divergence $\omega_b \approx 0.17$ sr) pulsed molecular beam was incident on a liquid-nitrogen cooled copper cold conduit and a multichannel plate attached to it. The 4-mm thick duraluminum plate had a close-packed array of channels with diameter $d_0 = 0.5$ mm and a hole pitch (center to center spacing) of 0.75 mm. The plate temperature measured with a thermocouple was $T_s \approx 80-85$ K. The distance between the nozzle cut and the plate surface was 93 mm. To rule out operation of the plate in a 'transparent' mode, it was rotated through angle $\alpha \geqslant 12^\circ$ with respect to the incident beam axis.

The authors of Ref. [127] experimented with molecules passing through a coolable hollow tapered truncated copper cone attached to the cold conduit instead of the multichannel plate (see Fig. 10). The inlet and outlet openings of the 25-mm long cone were 9 and 3.4 mm in diameter, respectively. In experiments on molecule reflection from the surface, the copper plate was attached to the cold conduit on the side of the incident molecular beam. A coolable diaphragm 4 mm in diameter was placed roughly 60 mm from the nozzle to extract a relatively narrow-directed beam of SF_6 molecules incident on the cooled plate. The nozzle and the plate surface were spaced 87 mm apart. The cold conduit with the attached plate was rotated through an angle of 80°. The molecules reflected from the surface were detected in the receiver (see below).

The molecular beam was produced using a pulsed 'current loop' type nozzle [133] with an orifice diameter of 0.75 mm. The nozzle-opening time varied from 70 to 100 μs (at the half-height of the opening pulse), depending on the gas composition and pressure above the nozzle. The gas pressure was varied from 0.1 to 6 atm. The nozzle was cut in the form of a 30-mm long cone with a whole vertex angle of 26°. The vacuum chamber in which the molecular beam was produced was pumped down to a pressure of about 3×10^{-6} Torr. The number of molecules outgoing from the nozzle in a single pulse depended on the above-nozzle pressure and varied from 8×10^{14} to 1×10^{17}. The method for measuring the number of molecules in a pulse was described at length in Refs [7, 123, 134]. The nozzle was operated either in the single-pulse mode or at a frequency repetition rate up to 1 Hz.

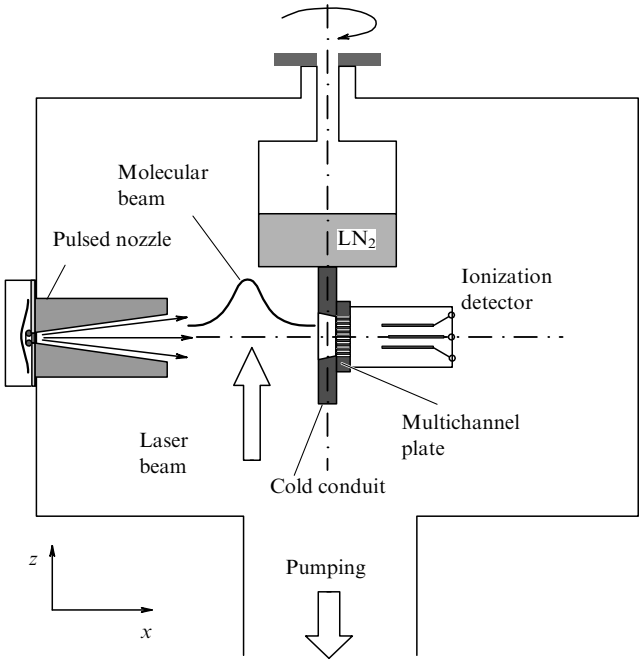

Figure 10. Layout of the experiment.

Molecular beam intensity I_b was evaluated in Refs [123, 134] from the measured number of molecules N_b in the beam, its duration τ_b, and divergence ω_b: $I_b = N_b/(\omega_b \tau_b)$. Beam duration measured with a pyroelectric detector [135, 136] at a distance of 90 mm from the nozzle (near the cold conduit surface) was $\tau_b \approx 150$ μs.

Molecules were vibrationally excited by intense (10^6 – 10^7 W cm^{-2}) radiation from a frequency-tuned pulsed CO_2 laser with a pulse energy up to 3 J. The laser beam intersected the molecular beam roughly 1.5–2.0 cm from the multichannel plate surface or the cone inlet orifice. The size of the laser spot in the excitation zone was around 10×10 mm^2. A double-pass scheme of molecular excitation in the beam was realized in most experiments. In this case, the laser beam intersected the molecular beam and reflected back at a small angle. This allowed exciting roughly twice as many molecules in the beam. A four-pass scheme of molecular irradiation was also employed in certain experiments with excitation of around 50–60% of the molecules in the incident beam.

Molecular layers on the surface and walls of the multichannel plate were formed by condensation of vibrationally 'cold' (unexcited) molecules of the incident beam. Note that in the presence of many molecules on the surface (i.e., more than one layer or over 10^{14} molecules/cm^2), they can arrange themselves into clusters [137]. The experimentation with rather intense pulsed molecular beams in Refs [125–128] created favorable conditions for the formation of a large number of molecular layers (over appr. 10–20) on the cold plate surface and the channel walls; they were realized even if a single pulse of the molecular beam or its forepart, the molecules of which were not exposed to laser radiation, fell on the multichannel plate.

Molecules passing through the multichannel plate and molecules of the starting beam were detected using an ion pressure gauge, namely, a PMI-2 tube, positioned so that the passing molecules were incident directly into the tube. Both the multichannel plate and the tube rotated about a common vertical axis (see Fig. 10), which allowed varying the angle of incidence α of the beam on the plate and thereby its transparency. Because a signal from the ionization tube is proportional to pressure or the number of molecules and independent of their vibrational energy, this method permits us to determine the relative number of molecules passing through the multichannel plate both in the case of laser excitation and without it. The ionization tube signal was fed to the VIT-2 psychometric hygrometer and the N307/1 recorder.

Molecules of the starting beam and molecules passed through the multichannel plate were also detected in Refs [125–128] by the pyroelectric method [7, 123, 135, 136]. It was also used to measure the energy absorbed by molecules from the laser pulse field. The pyroelectric detector and the ionization tube can rotate about the vertical axis common to the plate and the cone (see Fig. 10).

Also investigated was the dependence of the pyroelectric signal induced on the detector by molecules passing through the plate on the molecular beam parameters, on the laser pulse parameters, and on the beam incidence angle with respect to the plate. To improve the sensitivity of the method, molecules that passed through the plate were

excited by a second pulsed CO_2 laser, which allowed ascertaining exactly the passage of molecules through the multichannel plate and determining the fraction of the molecules that passed from the energy absorbed from the pulse of the second laser. The two detection methods yielded virtually similar results [125–127]. The data presented in Section 7.3 were obtained using a pyroelectric detector.

7.3 Results

7.3.1 Angular dependence of the probability of molecule passage through a multichannel plate and a cone. References [125, 126] were designed to study the passage of laser-excited and unexcited molecules through a cooled multichannel plate.

It was ascertained (Fig. 11a) that probability for vibrationally excited molecules to pass through the plate is much higher than that for unexcited molecules. Figure 11b shows the angle α dependence of the $\eta = I_L/I_0$ ratio of ion signals induced by SF_6 molecules that passed through the plate under conditions of molecular beam excitation (I_L) and in its absence (I_0). It can be seen that ratio η increases as the angle grows ($\alpha \geqslant 12°$); it reaches $\eta \approx 1.8$ at $\alpha = 22.5°$.

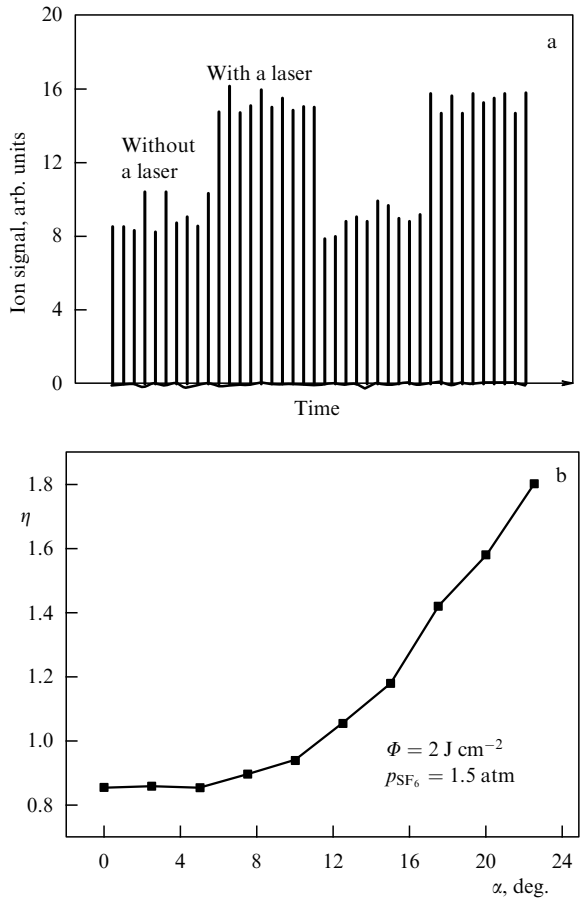

Figure 11. (a) Diagram illustrating the passage of SF_6 molecules in a beam through a multichannel plate cooled to $T_s \approx 80-85$ K under vibrational excitation by a laser pulse and in its absence. Beam incidence angle relative to the plate is $\alpha = 22.5°$. Exciting radiation frequency: 945.98 cm^{-1} (10P(18) line of CO_2 laser). Radiation energy density $\Phi = 2.0$ J cm^{-2}, and SF_6 pressure above the nozzle is 1.5 atm [128]. (b) Dependence of the signal ratio $\eta = I_L/I_0$ for SF_6 molecules passed through the multichannel plate on the beam incidence angle α relative to the plate in the case of vibrational excitation of molecules (I_L), and in its absence (I_0). Other experimental conditions are the same as in figure a [126, 128].

That the values of η are somewhat less than unity at small angles α is attributable to the dissociation of a small fraction of molecules and the ejection of the resultant fragments from the beam under the effect of employed laser radiation. At low excitation energy density, when molecules did not dissociate, η at small angles was equal to 1.

To recall, laser radiation in these experiments affected roughly one third of the molecules in the incident molecular beam. This means that at the pumping energies used in the experiments practically all molecules in the irradiated volume passed into high vibrational states [7, 123, 138], and probability P_L of the passage of highly excited molecules at $\eta \approx 1.8$ was roughly 3.4 times that of unexcited molecules:

$$\frac{2}{3} P_0 + \frac{1}{3} P_L = 1.8 P_0 ; \qquad (7.3)$$

whence, $P_L/P_0 = 3.4$.

Similar results were obtained in experiments on the passage of CF_3I molecules through a cooled tapered cone [127]. After exciting the vibrational mode ν_1 (frequency ≈ 1075.0 cm^{-1} [139]), molecules were passed through heated ($T_s \approx 295$ K) and cooled ($T_s \approx 80-85$ K) cones. In the latter case, at $\alpha = 0$, the signal was roughly 7.5 times weaker than in the former. Such a signal ratio is only slightly smaller than the ratio of the input and output orifice areas, $R = S_{in}/S_{out} \approx 9$, meaning, first, that most CF_3I molecules falling on the cold walls of the cone become trapped by them. Only those molecules that propagate within a solid angle given by outlet orifice dimensions and a small part of the molecules reflected from the cold walls pass through the cone. Second, practically all the molecules falling on the inlet orifice at $T_s \approx 295$ K and $\alpha = 0$ pass through the cone. At the same time, as angle α increases not all molecules entering the cone pass through it, even at $T_s \approx 295$ K; some of them are reflected by the walls and remain inside. Nonetheless, a rather large fraction of molecules do pass through the cone (over 50% at $\alpha = 30°$).

The behavior of CF_3I molecules in the cooled cone is altogether different. Figure 12 presents incidence angle α dependences of the ion signals induced by CF_3I molecules passing through heated (curve *1*) and cooled (curve *2*) cones, with the maximum signal values normalized to unity. As soon

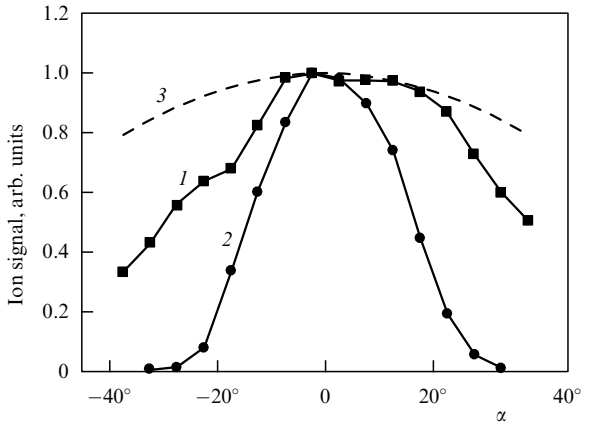

Figure 12. Incidence angle α dependences of the signals from CF_3I molecules that pass through heated (curve *1*) and cooled (curve *2*) cones. Maximum signal values are normalized to unity, for clarity. Curve *3* ($\cos\alpha$) is shown for comparison. Exciting radiation frequency: 1071.88 cm^{-1} (9R(10) line of the CO_2 laser). Energy density: 0.8 J cm^{-2}, and CF_3I pressure above nozzle: 2 atm [127, 128].

as the rotation angle of a cone reaches approximately 20 degrees ($\alpha \approx 19.5^\circ$ under the above experimental conditions), it is no longer 'transparent' for the incident particles and the probability (efficiency) of CF_3I passage sharply decreases. For $\alpha \geqslant 25^\circ$, fewer than 10% of the molecules pass through the cone. However, the efficiency of molecule passage through the cooled cone increases significantly after they are excited by a strong laser pulse [127].

7.3.2 Dependence of the probability of molecule passage through a multichannel plate on the starting beam intensity. Figure 13 demonstrates the dependence of ratio $\eta = I_L/I_0$ of ion signals induced by SF_6 molecules after passage through a multichannel plate following their excitation in the beam (I_L) and without excitation (I_0) on the molecular beam intensity I_b [125, 126]. Ratio η decreases with increasing intensity and becomes close to unity for $I_b \geqslant 10^{21}$ molecules per sr per s. Such behavior of η can be explained as follows. While the incident beam intensity is relatively low, the mean free path Λ of the molecules in the beam, defined by the relation $\Lambda \sim 1/n\sigma$ (where n is the SF_6 molecule concentration, σ is the gas-kinetic cross section of SF_6 collisions), is greater than the plate channel length, $\Lambda > L$. If the plate is operated in a nontransparent mode, virtually all passing molecules collide with the channel walls, with all or part of them being trapped by the cold walls. The probability of trapping is rather high. The influence of laser excitation is maximally pronounced just under these conditions. As the mean free path of molecules in the channels becomes shorter than their length and diameter ($\Lambda < L, d_0$) with a rise in incident beam intensity, the fraction of molecules that fail to collide with cold channel walls begins to prevail [140–142]; they lose the ability to be trapped. These molecules collide only with one another as they pass through the multichannel plate. Naturally, the probability of their passage no longer depends on molecular excitation. In a high-intensity beam, such molecules come to prevail, with the effect that the influence of laser excitation sharply decreases and disappears as beam intensity grows further.

The results presented in Fig. 13 indicate that maximum values of ratio $\eta = I_L/I_0$ are possible to obtain only if $\Lambda > L$. Therefore, the concentration of molecules in the beam under experimental conditions ($L = 4$ mm, $\sigma = 2.5 \times 10^{-15}$ cm^2) [143] must satisfy the condition $n \leqslant 10^{15}$ cm^{-3}, while the beam intensity must be $I_b \leqslant 2 \times 10^{21}$ molecules per sr per s. The total number of molecules flowing out from the nozzle must in this case be $N_b \leqslant 5 \times 10^{16}$ per pulse.

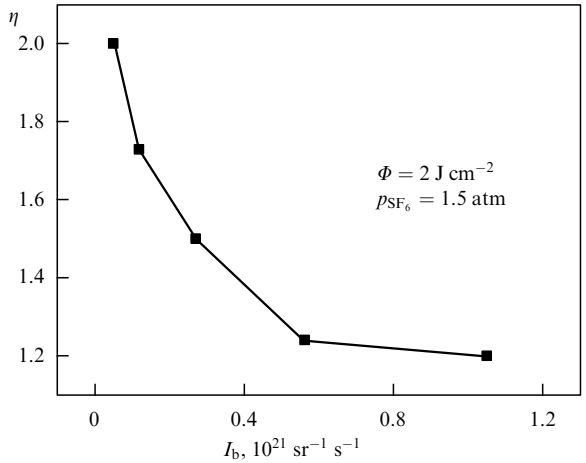

Figure 13. Dependence of the ratio of signals from SF_6 molecules that passed through a multichannel plate on molecular beam intensity with vibrational excitation and without it. See Fig. 11a [126] for other experimental conditions.

7.3.3 Dependence of the probability of molecule passage through a multichannel plate on exciting radiation energy density. Figure 14a illustrates the dependences of the ratio $\eta = I_L/I_0$ of ion signals induced by SF_6 molecules that passed through a multichannel plate, with molecular beam excitation (I_L) and without it (I_0), on exciting radiation energy density Φ. The dependences are presented for three excitation frequencies, viz., 949.5, 946.0, and 944.2 cm^{-1}, corresponding to the maximum, high-frequency, and low-frequency wings of the SF_6 multiphoton absorption spectrum of the pulsed molecular beam (see Section 7.4 and Fig. 15).

It follows from Fig. 14a that the efficiency of molecule passage through the plate grows considerably with exciting radiation energy density. This suggests a strong dependence

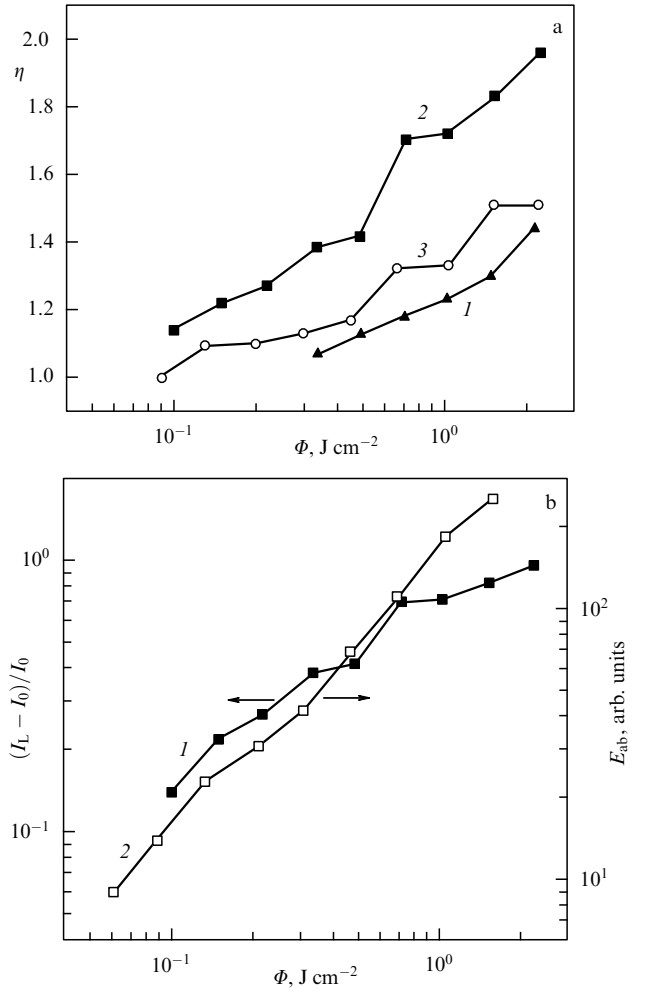

Figure 14. (a) Plots of the ratio of signals from SF_6 molecules that passed through a multichannel plate versus exciting radiation energy density for CO_2-laser lines with vibrational excitation and without it: 10P(14), $\nu = 949.5$ cm^{-1} (curve *1*); 10P(18), $\nu = 946.0$ cm^{-1} (curve *2*), and 10P(24), $\nu = 944.2$ cm^{-1} (curve *3*). (b) Plots of the relative number of SF_6 molecules that passed through the plate (curve *1*) and their absorbed energy (curve *2*) versus exciting radiation energy density. See Fig. 11a [126, 128] for other experimental conditions.

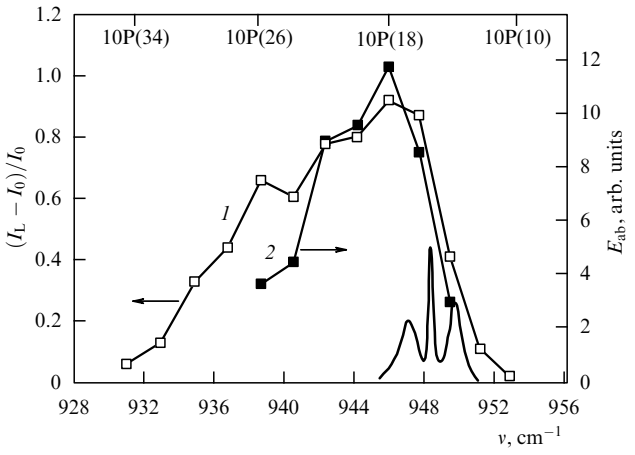

Figure 15. Spectral dependences of the relative fraction of vibrationally excited SF_6 molecules that passed through a multichannel plate (curve *1*) and of the energy absorbed by them (curve *2*). Experimental conditions are the same as in Fig. 11a [125, 128]. The thick curve at the bottom shows, for comparison, the linear absorption spectrum of excited SF_6 vibrational mode ν_3 in a gas-dynamically cooled molecular jet at $T \approx 55$ K [146].

of the probability of molecule reflection from the cold wall surface on the molecule vibrational energy. Thus, a maximum signal induced by SF_6 molecules passing through a cone was observed at the frequencies of the 10P(16) — 10P(24) band generation lines of a 10.6-μm CO_2 laser, i.e., in the frequency region 940–948 cm^{-1} characterized by maximum SF_6 absorption in the molecular beam [7, 123, 138]. By way of example, for molecular excitation at the 10P(16) line frequency (Fig. 14a), the mean energy absorbed by a single SF_6 molecule exceeds 1.5 eV at a laser energy density of 2.0 J cm^{-2} and 0.3 eV at an energy density of 0.4 J cm^{-2} [7, 123, 138]. The translational energy of SF_6 molecules in the beam in this experiment was $E_{tr} \approx 0.16$ eV [123, 144, 145].

A comparison of dependences of the relative fraction of molecules passing through the multichannel plate, $f = (I_L - I_0)/I_0$, and of the absorbed energy E_{ab} on the exciting radiation energy density Φ gives an insight into the role played by the vibrational energy in the passage of molecules through the cooled plate. It follows from Fig. 14b that these dependences are rather similar for energy densities $\Phi < 0.5$ J cm^{-2}. For higher energy densities, $\Phi \geqslant 0.6$–0.7 J cm^{-2}, when the mean energy absorbed by a molecule is roughly equivalent to 4–5 quanta of laser radiation (around 0.5–0.6 eV) [7, 136, 138], the fraction of molecules passing through the plate shows a weak dependence on Φ, whereas the absorbed energy continues to increase with Φ. This can be attributed to the fact that the passage needs only a certain amount of stored vibrational energy to occur. Once it is available, the probability of their passage ceases to further depend on the molecular energy.

7.3.4 Spectral dependence of the probability of molecule passage through a multichannel plate. It was ascertained in Refs [125, 126] that the efficiency of molecule passage through a cooled multichannel plate strongly depends on the laser exciting radiation frequency.

Figure 15 depicts the spectral dependences of the relative fraction of SF_6 molecules that passed through a multichannel plate with vibrational excitation (curve *1*) and of the molecular energy absorbed under the same conditions. The excitation energy density was $\Phi = 2.0$ J cm^{-2}. The dependences correlate fairly well. The total width of the spectral dependences at half height reaches about 10 cm^{-1}, much smaller than the isotope shift in the excited vibrational band ν_3 for $^{32}SF_6$ and $^{34}SF_6$ molecules (roughly 17 cm^{-1} [147, 148]). Therefore, the spectral dependences for the molecules passing through the plate give reason to suppose that the method of interest can be employed to select in a beam those molecules with the desired isotope (component) composition.

Table 1 presents some results of research on SF_6 and CF_3I molecule passage through a multichannel plate and a cone, and on reflection of these molecules from the surface [125–128]. It demonstrates a significant difference between the probabilities of the passage of excited and unexcited SF_6 and CF_3I molecules through the cone and of the reflection of relevant CF_3I molecules from the surface.

7.4 Discussion of results and conclusions

The enhanced probability of the passage of vibrationally excited SF_6 and CF_3I molecules through a multichannel plate and a cone derives from the fact [125–128] that the excited molecule energy is much higher than the molecular binding energy in clusters (for example, the binding energy of SF_6 and CF_3I molecules in clusters is roughly 0.29 and 0.36 eV, respectively [137, 149]). As a result, the probability of reflection of vibrationally excited molecules from a molecule-coated surface is higher than that of unexcited ones.

The results thus obtained suggest that the above-described method can be applied to separate excited and unexcited molecules in a beam. Naturally, the optimal conditions for this purpose would be the reflection of only excited molecules from the surface, with all unexcited ones being trapped and undergoing no desorption. Meanwhile, the available data indicate that unexcited molecules are also quite effectively reflected (scattered) from the surface and pass through a multichannel plate and a cone due to the following.

First, the probability of molecular trapping under the above experimental conditions is other than unity because the surface has a rather high, not zero, temperature, and the

Table 1. Results of experiments on excited and unexcited SF_6 and CF_3I molecule passage through a multichannel plate and a cone, and on their reflection from the surface [128].

Molecule	Interaction surface	Laser line	Φ, J cm^{-2}	Portion of irradiated molecules	α, deg.	I_b, 10^{20} sr^{-1} s^{-1}	$\eta = I_L/I_0$	P_L/P_0
SF_6	Multichannel plate	10P(18)	2.0	0.5	22.5	0.5	2.0	3.0
SF_6	Cone	10P(18)	2.6	0.5	35	1	2.7	4.4
CF_3I	Cone	9R(12)	0.9	0.5	35	3	2.7	4.4
CF_3I	Plate	9R(10)	1.5	0.5	≈ 80	1	5.3	9.6

energy of molecules in the incident beam (including unexcited ones) is rather high. Suffice it to say that the mean kinetic energy of SF_6 and CF_3I molecule in the incident beam is roughly 0.16 and 0.17 eV, respectively [123, 144, 145]. The vibrational energy of SF_6 beam molecules was estimated to be $E_{vib} \approx 0.02$ eV [128] at $T_{vib} \approx 150$ K [123, 135, 136], The rotational energy of molecules in the beam can apparently be neglected, because their rotational temperature is much lower than the vibrational one ($T_{rot} \leqslant 30$ K) [7,123, 135, 136].

Second, the adsorbed molecules are very likely to desorb by virtue of the rather high surface temperature. These causes appear to lie behind the ability of unexcited molecules to pass, with a high enough probability, through multichannel plates and cones and be reflected from their surfaces, meaning that the energy of molecules in an incident beam should be decreased if selectivity of the process is to be enhanced as reported in Refs [140–142]. In addition, the surface on which the molecules are to be condensed needs to be deeply cooled. It is worthwhile to note, however, that it may decrease the probability of both reflection of excited molecules from the surface and their passage through a plate or a cone (see below).

Let us compare the results of papers [125, 126] with the data considered in Section 2 and reported in Refs [31, 32] concerning the role of translational and vibrational energies of SF_6 molecules in a continuous beam during its reflection from a cold surface. To recall, translational and vibrational energies in Refs [31, 32] were varied within narrow limits by heating the nozzle. It was ascertained that the reflection coefficient for vibrationally excited molecules is several times that for unexcited ones only when their translational energy is low (less than 0.04 eV). At a translational energy in excess of 0.15 eV, the reflection coefficients for excited and unexcited molecules were virtually identical. The above studies were carried out at a surface temperature of ~ 50 K, when the total fraction of the surface-reflected molecules was below 1%.

Worthy of note are the studies reported in Refs [31, 32], and those considered in Section 2 were conducted under conditions in which molecules had small vibrational energy reserves (below 0.12 eV), because their excitation by a continuous CO_2 laser or nozzle heating did not induce population of high vibrational levels. As a result, the influence of vibrational excitation on the processes of interest was insignificant. One essential difference in experiments [125–128] consists in the fact that they involved strongly excited molecules having a vibrational energy in excess of about 0.3–1.5 eV. Relaxation of vibrational excitation at such high energies requires a large number of collisions to occur, i.e., it takes more time. Another essential difference is that the molecules' vibrational energy in Refs [125–128] was much higher than the molecular binding energy in clusters and the molecule–surface binding energy (equal roughly to 0.2–0.3 eV). This fact possibly accounts for the appreciable difference in the probability of passage of excited and unexcited molecules through the multichannel plate or the cone and the probability of their reflection from the surface (see Table 1). For example, some 5–7% of the incident molecules passed through the plate at $\alpha = 17.5^\circ$ and $\eta \approx 1.4$ (Fig. 11b). An even higher passage efficiency was documented in paper [127], where a tapered cone was utilized instead of a multichannel plate. At small excitation energy densities, the influence of the molecules' internal energy on their passage efficiency was insignificant (Fig. 14a).

Thus, experiments reported in Refs [125–128] demonstrate that SF_6 and CF_3I molecules excited in a beam by intense IR laser radiation and thereby transferred to high vibrational states with energies on the order of $0.3 \leqslant E_{vib} \leqslant 2.0$ eV much more efficiently pass through multichannel plates and cones cooled to $T_s \approx 80-85$ K and also reflect off the molecule (cluster)-coated surface than unexcited molecules.

It has been established that the probabilities of molecule passage through plates and cones and reflection from surfaces strongly depend on the energy density and the frequency of the laser exciting pulse. This opens up possibilities to apply these processes for laser-assisted selection of molecules in a beam in terms of their isotope and/or component compositions. Further investigations are, however, needed to evaluate the selectivity and efficiency of the relevant processes.

8. Isotope separation involving clusters and nanoparticles

Some recent studies [150–153] have dealt with isotope separation involving clusters and nanoparticles. It was proposed [150, 151] to utilize molecular trapping and subsequent transport by large clusters (nanoparticles) in intersecting molecule and cluster beams. To this end, the authors of Refs [152, 153] used disintegration of weakly bound van der Waals clusters upon collisions with highly vibrationally excited molecules. Let us consider the basic ideas behind these approaches and their results in the context of application to molecular laser isotope separation.

8.1 Laser control of molecule capture by large clusters (nanoparticles)

The probability of trapping a molecule by a cluster or a cold surface (see Section 2.1) depends on the total energy of the molecule E_{tot} and the molecule–cluster binding energy E_b. Given that the energy of the molecule is small (lower than E_b), i.e., $E_{tot} < E_b$, it is very likely to be captured by the cluster–molecule interaction potential and taken away by the cluster. If, however, the total energy of the molecule is higher than the binding energy, $E_{tot} > E_b$, it may overcome the potential interaction barrier and be reflected from the cluster surface. In fact, both adsorption and desorption of the molecule on the cluster surface occur. The probability of desorption P_{des} is defined in Refs [21, 129] by a relation analogous to formula (7.2):

$$P_{des} \sim \exp\left(-\frac{E_b}{E_{tot}}\right). \tag{8.1}$$

This means that the probability of trapping the molecule preliminarily excited in a beam by intense IR laser radiation is much lower than that of an unexcited molecule. IR multiphoton absorption makes it possible to introduce a rather high energy (commensurate with the molecule dissociation energy) into vibrational degrees of freedom. Vibrationally excited molecules are more likely to desorb from the cluster surface than unexcited ones. It is this difference that was documented in the experiments described in Refs [150, 151].

8.1.1 Experiment and method. Figure 16 illustrates the essence of the method. An intense pulsed cluster beam of Xe_N particles was intersected by an SF_6 molecular beam at a right angle. The molecules were trapped by Xe_N clusters in the

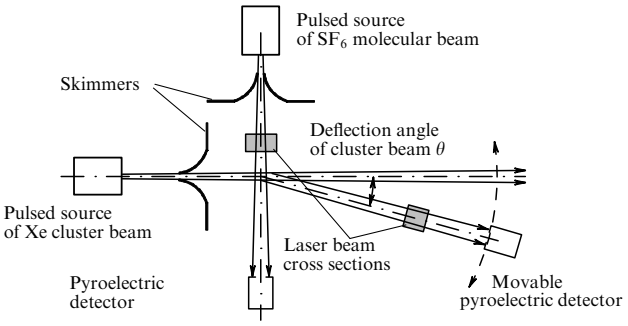

Figure 16. Layout of the experiment [150].

intersection region and transferred a momentum to them [97, 122, 154] that made the clusters deflect at a certain angle. The source of the cluster beam was a pulsed 'current loop' type nozzle [133] of diameter about 0.75 mm and a nozzle-opening pulse duration (at half height) of about 120 μs. The nozzle was cut to be shaped like a 30-mm long cone with a whole vertex angle of 26°. The gas pressure above the nozzle varied from 0.5 to 4.5 atm. The formation of cluster beams in the pulsed nozzle was studied in considerable detail in Ref. [155]. In the above experiments, Xe_N clusters with $N \geqslant 10^2 - 10^3$ particles were generated. These large Xe_N clusters had a solid-state structure [156, 157].

A General Valve type pulsed nozzle (electromagnetic valve) with an opening diameter of 0.8 mm and nozzle-opening pulse duration (at half height) of about 300 μs was employed to produce an SF_6 molecular beam. The gas pressure above the nozzle varied from 0.5 to 2.5 atm. The cluster and molecular beams were extracted from pulsed jets generated with the aid of above-noted nozzles using conically shaped diaphragms (skimmers) with inlet orifice diameters of 3 and 6 mm placed at distances 30 and 26 mm from the nozzles, respectively. Uncooled pyroelectric detectors (PEDs) with a time resolution of 5–10 μs were used to detect the two beams [135, 136]. They were placed at different distances from the nozzles. The vacuum chamber in which the beams formed was pumped down to a pressure of $\approx 3 \times 10^{-6}$ Torr.

Intense CO_2-laser pulses were applied to vibrationally excite molecules in the beam. Specifically, free SF_6 molecules were excited by an IR 'pumping' pulse prior to their interaction with the cluster beam and molecules incorporated in Xe_N clusters by a 'probe' IR pulse after the interaction of beams. The excitation energy in the pulse amounted to 3 J, and its half-height duration was roughly 100 ns. In both cases, the laser radiation excited an active ν_3 vibrational mode of the molecules (948 cm^{-1}) in the IR region [147]. The molecular excitation was investigated by the pyroelectric method for the detection of the absorbed energy [7, 123, 135, 136]. The signal from molecular and cluster beams recorded by PEDs was amplified roughly 100 times and fed into a Tektronix TDS-1002 digital oscillograph. The beams operated in a single-pulse mode. Signals from the detector were averaged over 16 pulses.

The angle of cluster deflection during molecule trapping is given by the relation

$$\tan\theta = \frac{\sin\alpha}{m_1 v_1 / m_2 v_2 + \cos\alpha}, \qquad (8.2)$$

where m_1, m_2 and v_1, v_2 are cluster and molecule masses and velocities, respectively, and α is the angle between cluster and molecular beams. In the experiments being considered ($\alpha = 90°$, $m_2 \approx 146$ a.m.u.; $v_1 \approx 300$ m s^{-1} and $v_2 \approx 430$ m s^{-1} are the measured velocities of clusters and molecules in the beams), Xe_N clusters containing $N = 100$ or $N = 1000$ particles were each deflected through angles $\theta \approx 1°$ and $\theta \approx 0.1°$, respectively, as they trapped single SF_6 molecules.

The lifetime τ of an SF_6 molecule on the Xe_N-cluster surface depended on SF_6 sublimation (desorption) energy and Xe_N-cluster temperature. This can be estimated from a relation analogous to formula (7.1) [158]:

$$\tau = \tau_0 \exp\left(\frac{E_{\rm des}}{k_{\rm B} T_{\rm cl}}\right), \qquad (8.3)$$

where τ_0 is the molecule vibration period on the cluster surface with respect to the van der Waals bond, $E_{\rm des}$ is the sublimation or desorption energy per molecule, and $T_{\rm cl}$ is the cluster temperature. Reference [150] presents estimates based on the literature data for the parameters of relation (8.3): $\tau_0 \approx 10^{-13}$ s [157], $E_{\rm des} = 5.46$ kcal mol^{-1} [159], $T_{\rm cl} \approx 80$ K [156, 157]. They indicate that lifetime τ varies from several to tens of seconds. The estimates were made taking into account a weak heating of the clusters (by roughly 7.5 K for an Xe_{100} cluster) at the expense of the SF_6 kinetic energy in the molecular beam (of about 0.16 eV [123]), meaning that SF_6 molecules fail to sublimate from the cluster surface for the time that the cluster beam needs to reach the detector (≈ 500 μs). Excitation of SF_6 molecules incorporated in the clusters by IR laser probe pulses generates an additional signal in the receiver detecting the cluster beam [160, 161] (Fig. 17b, signal S_1).

When SF_6 molecules are excited by an IR laser pump pulse before interaction with the cluster beam (see Fig. 16), their energy after attachment to the cluster is rapidly (in a time $\leqslant 1$ ps) transferred onto the clusters. Cluster temperature grows significantly, which markedly increases the probability of SF_6 sublimation (desorption) from the cluster surface. For example, if an SF_6 molecule incorporated into an Xe_{100} cluster has the vibrational energy $E_{\rm vib} \approx 1$ eV, its relaxation results in a $\Delta T \approx 46$ K rise in cluster temperature to $T_{\rm cl} \approx 126$ K. Then, the probability of molecule sublimation from the cluster surface increases, in accordance with formula (8.1), more than threefold. The lifetime of an SF_6 molecule on the cluster surface will roughly be 50 μs. Molecules that sublimated from the Xe_N cluster surface travel in the laboratory reference frame toward the cluster beam inside a rather wide solid angle determined by the molecule velocity (kinetic energy), i.e., cluster temperature [160, 161]. This leads to a considerable depletion of the signal from the receiver detecting the cluster beam if molecules and doped clusters are sequentially exposed to pump and probe laser pulses (Fig. 17c, signal S_2).

Let us recall that PED detection of the beams of molecules with energy $E_{\rm tot}$ satisfying the condition $E_{\rm tot} > k_{\rm B} T_{\rm s}$ (where $k_{\rm B} T_{\rm s}$ is the surface energy of the active detector element) induces a positive signal. In contrast, a negative signal is induced if low-energy molecular beams ($E_{\rm tot} < k_{\rm B} T_{\rm s}$) and cluster beams are detected by the PED [155]. The generation of negative signals during detection of cluster beams is due to the fact that clusters dissociate in collisions with the PED surface and the energy needed for their dissociation is taken from the detector surface. Thus, xenon atoms and clusters induce signals on PEDs with positive and negative polarities [155].

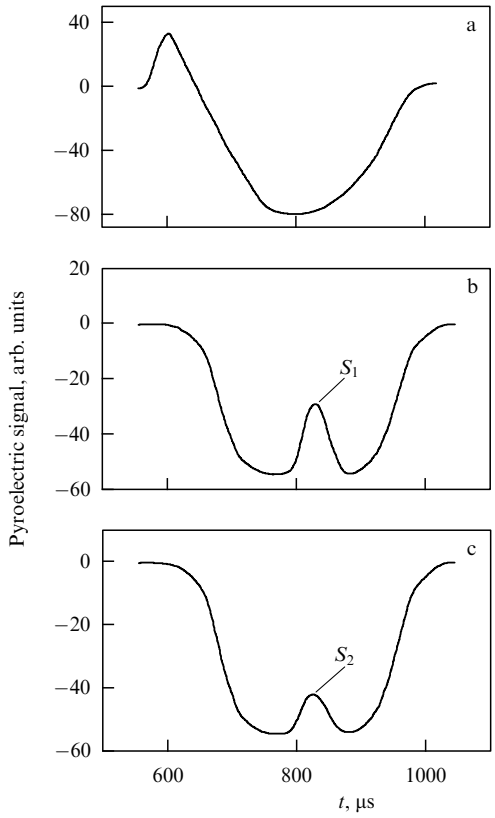

Figure 17. Signals induced in a pyroelectric detector positioned at angle $\theta \approx 1°$: (a) in the absence of a molecular beam, (b) by an Xe_N cluster beam with trapped SF_6 molecules excited by a CO_2-laser 'probe' pulse alone, and (c) by an Xe_N cluster beam with trapped SF_6 molecules excited first by a 'pump' pulse of the first CO_2 laser and then by a 'probe' pulse of the second CO_2 laser. The Xe and SF_6 gas pressures above the nozzles were 4 and 2 atm, respectively. The nozzle and the receiver detecting a cluster beam were spaced 205 mm apart. Radiation frequencies of the 'pump' and 'probe' pulses were 946 cm^{-1} (laser generation line 10P(18)). Pulse energy density $\Phi_1 = \Phi_2 = 1$ J cm^{-2} [150].

8.1.2 Results and their analysis. Figures 17a–c show, respectively, signals induced on a detector positioned at angle $\theta \approx 1°$ by a Xe_N cluster beam in the absence of a molecular beam, an Xe_N cluster beam containing trapped molecules excited only by a CO_2-laser probe pulse, and a Xe_N cluster beam with captured SF_6 molecules preliminarily excited by the pump pulse of the first CO_2 laser and subsequently excited by the probe pulse of the second CO_2 laser.

It follows from Fig. 17a that xenon atoms and clusters induce in PEDs signals differing in polarity as described in Ref. [155]. The 'atomic constituent' of the Xe beam (positive signal) practically disappears in the presence of an SF_6 beam (Fig. 17b, c), because both molecules and small clusters become deflected at larger angles. Figure 17b demonstrates that a negative signal from Xe_N clusters is induced on the detector together with a positive signal (S_1) resulting from excitation of SF_6 molecules incorporated in the clusters by the CO_2-laser probe pulse. The signal induced on the detector is much weaker when SF_6 molecules are preliminarily (before interaction with the cluster beam) excited by the laser pulse as well (Fig. 17c, signal S_2). This means that a correlation between S_1 and S_2 signal amplitudes may be utilized to evaluate the effectiveness of the trapping of vibrationally excited and unexcited SF_6 molecules by a cluster beam, while

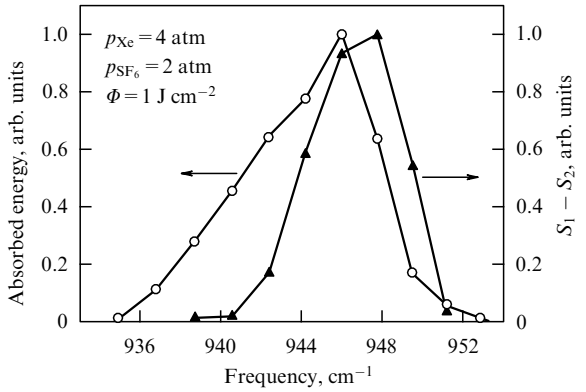

Figure 18. Dependence of $S_1 - S_2$ signal difference on the frequency of the SF_6-exciting CO_2-laser pump pulse (triangles, right y-axis) and frequency dependence of the SF_6-absorbed energy of the laser pump pulse, i.e., the MPA spectrum of SF_6 in the molecular beam (circles, left y-axis). The maximum signal values are normalized to unity, for clarity. See Fig. 17 for other experimental conditions [150].

variations of the frequency and energy density of the exciting CO_2-laser pump pulse make it possible to obtain spectral and energy characteristics of the efficiency of trapping the vibrationally excited molecules by clusters.

Figure 18 plots the dependence of signal difference $S_1 - S_2$ on the frequency of the SF_6-exciting CO_2-laser pump pulse. For comparison, the frequency dependence of the SF_6-absorbed energy of the laser pulse field, i.e. the multiphoton absorption spectrum of SF_6 in the molecular beam, is presented. The two dependences are in excellent correlation. This finding indicates that molecule trapping by clusters is highly sensitive to the vibrational energy of the molecules, which implies that vibrationally excited molecules are far less effectively trapped than unexcited ones. The correlation between the spectral dependence of $S_1 - S_2$ and the multiphoton SF_6 absorption spectrum also suggests that such an approach can be utilized for isotope separation by taking advantage of the presence of an isotope shift in the spectra of irradiated molecules.

Figure 19 depicts the dependence of the signal ratio S_1/S_2 on the energy density of the SF_6-exciting laser pump pulse at a frequency of 946 cm^{-1} (10P(18) laser generation line). The S_1/S_2 ratio grows with energy density and amounts to $S_1/S_2 \approx 4$ at $\Phi \approx 2$ J cm^{-2}. It is worthy of note that the S_1/S_2 ratio strongly depends on the portion of molecules interacting with the exciting laser pulse at a given energy density. Earlier studies [7, 136] showed that the portion of SF_6 molecules interacting with the exciting laser pulse in an irradiated volume at the energy density $\Phi \approx 2$ J cm^{-2} approaches $f \approx 0.75-0.8$. Since the S_1/S_2 quantity is given by the relation

$$\frac{S_1}{S_2} \leqslant \frac{1}{1-f}, \tag{8.4}$$

the above values of $S_1/S_2 \approx 4$ at $\Phi \approx 2$ J cm^{-2} and $S_1/S_2 \approx 2.3$ at $\Phi \approx 1$ J cm^{-2} are consistent with the expected values for the earlier measured values of $f \approx 0.75-0.80$ and $f \approx 0.5-0.6$ at the specified energy densities [7, 136]. Consequently, this result also suggests sublimation of practically all vibrationally excited SF_6 molecules from the Xe_N cluster surface in the time needed to reach the detector.

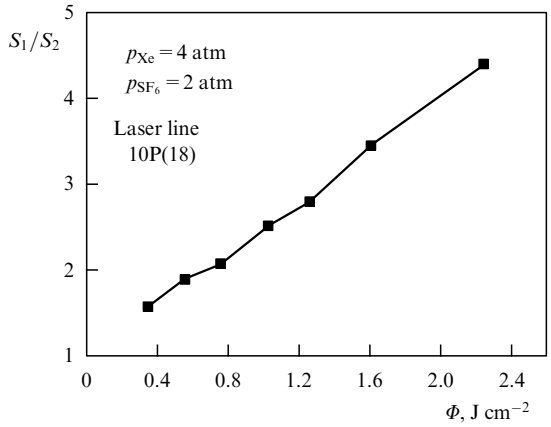

Figure 19. Signal ratio S_1/S_2 vs energy density of the SF_6-exciting CO_2-laser pump pulse. Frequency is 946 cm^{-1} (10P(18) line). Energy density of the probe pulse is $\Phi_2 = 3$ J cm^{-2}. See Fig. 17 for other experimental conditions [150].

To sum up, Refs [150, 151] have demonstrated that intense IR laser radiation can be employed to control the trapping of chromophore molecules by cold nanoclusters of noble gases in intersecting cluster and molecular beams.

A drawback of the proposed method from the standpoint of achieving the high selectivity comes from the difficulty of exciting all the molecules present in the beam, i.e., the difficulty of creating conditions under which $f \approx 1$ not only in the irradiated volume but also in the entire 'bunch' of a pulsed molecular beam. All molecules can only be excited by exploiting very short pulsed molecular beams ($\leqslant 20$ μs at half-height) at a high energy density, as described, for example, in Refs [162, 163].

Analysis of the available data leads to the conclusion [150, 151] that the trapping of vibrationally excited molecules by clusters is a more complicated process, because the lifetime of a trapped molecule strongly depends on its vibrational excitation energy and therefore on the temperature to which the molecule can 'heat' the cluster [see relation (8.3)]. Cluster heating causes SF_6 molecules and/or Xe atoms to evaporate (desorb). The relationship between the probabilities of desorption of these particles depends on the relationship between particle–medium binding energies in the cluster. Estimates show that at the level of SF_6 excitation achieved in the 'pumping' region of a given experiment the excited molecules trapped by the clusters have no time to reach the detector. At the same time, capture cross sections of the excited and unexcited molecules by clusters (in the 'gas-kinetic' sense) are either similar or equal, while the lifetimes of excited and unexcited molecules on the cluster are significantly different [150].

In the context of the application of molecule trapping by clusters for laser isotope separation, the foregoing implies that a cluster beam in the laboratory reference frame is enclosed inside a 'cone' formed by excitable target molecules (and possibly cluster atoms), whereas nontarget molecules remain inside the cluster beam. This observation should be taken into consideration when designing a spatial molecule separation process. It is worthwhile to note that the cone angle and particle composition (molecules, cluster particles) inside it depend on many factors, such as the particle binding energy, initial molecular energy, and particle mass. This issue may be the subject of further research.

8.2 Selection of molecules via cluster disintegration

It was shown in Refs [152, 153] that collisions of vibrationally excited SF_6 molecules with an energy of $E_{vib} \approx 0.5-2.0$ eV and weakly bound van der Waals clusters of Ar_N, Kr_N, and $(N_2)_N$ ($N \leqslant 30-40$) in intersecting molecule and cluster beams result in the trapping of molecules by clusters, with subsequent cluster disintegration and liberation of the trapped molecules. In principle, the process discovered and investigated in Refs [152, 153] can be employed to separate isotopes. Let us consider the experimental conditions and the rationale for the proposed method.

8.2.1 Experiment and the essence of the method

Experiment. The experimental setup used in Refs [152, 153] is analogous to that depicted in Fig. 16 and described in Section 8.1.1. An intense beam of Ar_N, Kr_N, or $(N_2)_N$ clusters intersected a pulsed SF_6 molecule beam at a right angle. The clusters trapped the molecules in the $L \approx 2$-cm long intersection region and were deflected through an angle given by relation (8.2). Under the experimental conditions of Refs [152, 153] ($\alpha = 90°$, $m_2 \approx 146$ a.m.u., $v_1 \approx 580$ m s^{-1} and $v_2 \approx 430$ m s^{-1} are the measured velocities of Ar_N clusters and SF_6 molecules in the beams), Ar_N clusters with $N = 15$ particles trapped individual SF_6 molecules and were deflected through the angle $\theta \approx 10°$, while those with $N = 30$ were deflected through the angle $\theta \approx 5°$. Krypton and nitrogen clusters with $N = 15$ became deflected through the angles $\theta \approx 4.8°$ and 14°, respectively.

This process was characterized by the Poisson distribution for a multiple capture [111, 121]. The probability of capturing k SF_6 molecules by one and the same cluster is determined by the probability of independently capturing k molecules, defined in Ref. [121] by the distribution

$$I_k = k_{k0} \frac{(n\sigma L)^k}{k!} \exp(-n\sigma L), \tag{8.5}$$

where k_{k0} is the amplitude factor, n is the gas particle number density, σ is the capture cross section, and L is the length of the interaction region. In the spherical particle approximation, the capture cross section is defined as

$$\sigma = \pi(r_{cl} + r_m)^2, \tag{8.6}$$

where $r_{cl} = r_0 N^{1/3}$ is the radius of a cluster with N atoms, r_0 is the van der Waals radius of an individual atom in the cluster, and r_m is the molecule radius. If the argon atom radius is assumed to be $r_0 = 1.92$ Å and the SF_6 molecule radius $r_m = 2.66$ Å [164], the cross section of an SF_6 capture by an Ar_{50} cluster is $\sigma = 9.5 \times 10^{-15}$ cm^2. The concentration of molecules in this region must be no less than $n \approx 5.3 \times 10^{13}$ cm^{-3} (or the effective pressure no less than 1.5×10^{-3} Torr) to enable an Ar_{50} cluster running through the interaction region ($L = 2$ cm) to capture at least one molecule. Such conditions were realized in experiments [152, 153].

Molecule and cluster beams were generated with pulsed nozzles described in Section 8.1. The source of the cluster beams was a 'current loop' type pulsed nozzle [133] with an orifice diameter of 0.75 mm and nozzle-opening pulse duration (at half height) of 120 μs. The nozzle was cut in the shape of a 32-mm long cone with a whole vertex angle of 18°. Gas pressure above nozzle varied from 0.5 to 5.5 atm. The cluster size depended on the above-nozzle gas pressure. Ar_N

clusters, each with $N \geqslant 10^2$ particles on the average, were generated at an above-nozzle gas pressure of $\geqslant 4$ atm. However, the beams thus obtained contained many clusters with $N \leqslant 50$ due to the nonuniform distribution of atomic concentrations in pulsed beams and the wide distribution of clusters by size. Under the same gas pressure above the nozzle, bigger clusters formed in krypton, and smaller ones ($N \leqslant 10^2$) in nitrogen [155]. Both molecular and cluster beams and the pulsed CO_2 laser exciting SF_6 molecules were synchronized so that all the excited molecules interacted with the clusters at the leading edge of the cluster beam pulse containing the largest portion of small clusters ($N \leqslant 50$).

Method. Let us consider the basic ideas behind the method, as exemplified by the trapping of SF_6 molecules by Ar_N clusters described in Refs [152, 153]. A molecule trapped by the cluster in a time $\leqslant 1$ ps transfers to the cluster an energy that heats it. The heated cluster cools via evaporation of atoms and trapped molecules [157, 165]. Vibrational predissociation takes place in a cluster. When the atomic binding energy E_b inside the cluster is significantly smaller than that of the trapped molecules with the cluster atoms ($E_b(\mathrm{Ar}-\mathrm{Ar}) \ll E_b(\mathrm{Ar}-\mathrm{SF_6})$), the cluster cools mainly due to the evaporation of its own atoms, while the trapped molecules are the last to disengage. It is such the process that was realized in Refs [152, 153], where SF_6 molecules were trapped by argon, krypton, and nitrogen clusters characterized by a relatively low atomic binding energy (see below).

These experiments were designed to elucidate the dependences of SF_6-absorbed energy $E_{ab}(\Phi)$ on energy density Φ of the exciting CO_2-laser pulse before the collision with Ar_N clusters and after their disintegration, $E_{res}(\Phi)$. In the general case

$$E_{res}(v, \Phi) = E_1 + E_{ab}(v, \Phi) - E_{cl.\,des}(N) - E_{cl.\,fr}\,, \qquad (8.7)$$

where E_1 is the total SF_6 energy (the sum of the kinetic, rotational, and vibrational energies) before laser excitation, $E_{ab}(v, \Phi)$ is the energy absorbed by a molecule from a laser pulse, $E_{cl.\,des}(N)$ is the energy needed to disintegrate an Ar_N cluster, and $E_{cl.\,fr}$ is the energy of the resultant cluster fragments.

The specific sublimation energy of an argon atom in macroscopic matter is $E_{subl} = 0.080$ eV, and its specific evaporation energy at boiling temperature is $E_{ev} = 0.068$ eV [166, 167). Analogous values are lower in small argon clusters, because the atomic binding energy in clusters decreases with decreasing the cluster size [119, 157]. For example, the atomic binding energy in an argon dimer is roughly 0.01 eV [168]. On the other hand, the evaporation energy of a few residual argon atoms in an SF_6/Ar_N cluster is close to the SF_6–Ar bond breaking energy (about 0.1 eV) [169]. However, this does not lead to a significant increase in the total energy needed to destroy rather big ($N \approx 10-40$) clusters. Therefore, it can be assumed that the disintegration energy of a cluster with size N satisfies the condition

$$E_{cl.\,des}(N) \leqslant N E_{cl.\,subl}(N)\,, \qquad (8.8)$$

where $E_{cl.\,subl}(N)$ is the energy of argon atom sublimation from the surface of a cluster with N atoms. At the same time, the following condition is fulfilled:

$$E_{cl.\,subl}(N) \leqslant E_{subl} = 0.080 \text{ eV}\,. \qquad (8.9)$$

Disintegration of an Ar_N cluster is possible when the total energy of a trapped SF_6 molecule satisfies the condition

$$E_{tot}(SF_6) = \left(E_1 + E_{ab}(v, \Phi)\right) \geqslant E_{cl.des}(N)\,. \qquad (8.10)$$

It follows from the foregoing that if the total energy of the trapped SF_6 molecule is lower than the Ar_N cluster disintegration energy, all the molecule's energy is spent to destroy the cluster. However, disintegration of the cluster is incomplete, the kinetic energy of its fragments is small (since the cluster temperature is low), and therefore a positive signal is not induced on the detector (see Section 8.1.1). Complete disintegration of an argon cluster occurs when the energy absorbed by SF_6 molecules from the laser field is high and the following condition is fulfilled:

$$E_{tot}(SF_6) \gg E_{cl.des}(N)\,. \qquad (8.11)$$

If energy E_2 of the released SF_6 molecules exceeds the surface energy of the detector's active element ($E_2 > k_B T_s \approx 0.025$ eV), a positive signal is, however, induced [155], as revealed in experiments [152, 153]. The SF_6-absorbed energy being dependent on the laser exciting radiation frequency, the PED signal at different excitation frequencies (laser generation lines) begins to be induced at different excitation energy densities (Fig. 20b).

8.2.2 Results and their analysis. Figure 20a plots the dependences of SF_6-absorbed energy $E_{ab}(\Phi)$ in the beam on exciting radiation energy densities for certain CO_2-laser generation lines coincident with the maxima in the SF_6 IR multiphoton absorption (MPA) spectrum [10P(18) line — 945.98 cm^{-1}], as well as with the low- and high-frequency wings of the MPA spectrum [10P(22) line — 942.38 cm^{-1} and 10P(14) line — 949.48 cm^{-1}, respectively]. The dependences have a relatively smooth power-like character. The energy absorbed by SF_6 grows almost monotonically with a rise in excitation energy density. Such a character of energy accumulation by molecules was observed in many earlier studies [7, 123, 136, 170] concerned with IR multiphoton excitation of SF_6.

The dependences of $E_{res}(\Phi)$ obtained in experiments with Ar_N clusters for the same laser radiation lines presented in Fig. 20b [152, 153] exhibit a totally different character. At low excitation energy densities, the energy E_{res} is practically nil for all the above lines. It sharply increases with increasing excitation energy density only on 10P(18) for $\Phi \geqslant 0.2$ J cm^{-2}, on 10P(22) for $\Phi \geqslant 0.4$ J cm^{-2}, and on 10P(14) for 0.7 J cm^{-2}. In fact, dependence $E_{res}(\Phi)$ shows a threshold character that can be accounted for by the emergence of SF_6 molecules in the cluster beam, released as a result of cluster disintegration. At excitation energy densities in excess of the above threshold values of Φ_{th}, i.e. for $\Phi > \Phi_{th}$, the energy of the released molecules is high enough to induce a positive detector signal. The signal rapidly grows with excitation energy density, because an increasingly bigger portion of the absorbed energy remains in the molecules after cluster disintegration. In this case, atom evaporation from the clusters containing captured vibrationally excited molecules can actually be regarded as relaxation of the excited SF_6 state. The energy relaxation process ends after complete cluster disintegration and disappearance of the energy relaxation channel.

It follows from the above results that the width of the spectral dependence $E_{res}(v)$ at a fixed excitation energy density of SF_6 molecules will be much smaller than that of

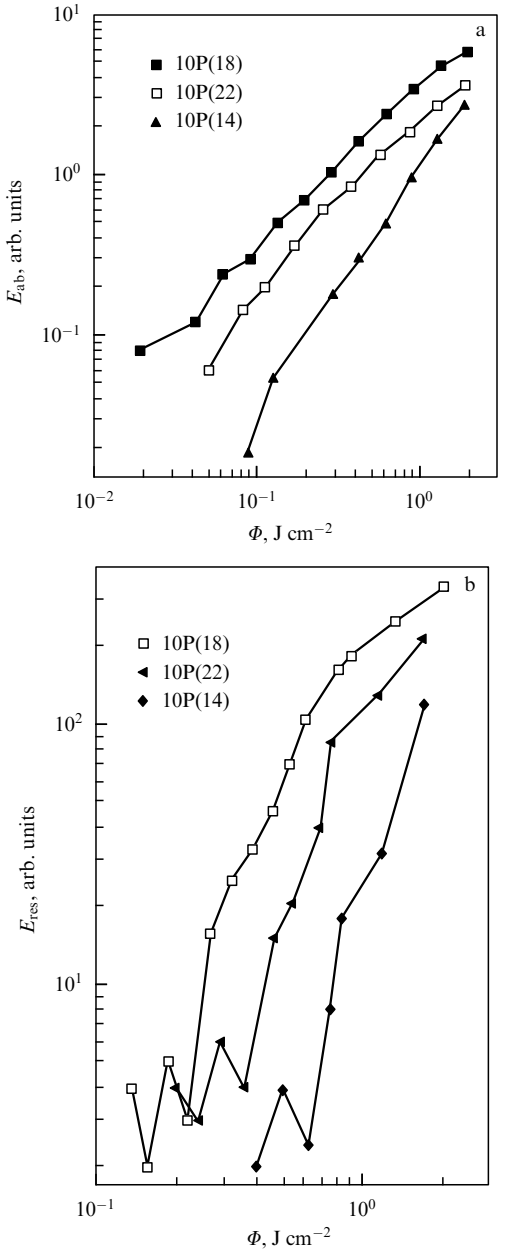

Figure 20. Plots of SF_6-absorbed energy in the beam E_{ab} (a) and residual (after cluster disintegration) energy E_{res} in SF_6 molecules (b) versus laser exciting radiation energy density Φ for 10P(18), 10P(22), and 10P(14) CO_2-laser generation lines. The pressure of Ar and SF_6 gases above the nozzle are 4.3 and 1.75 atm, respectively. The nozzle and the detecting receiver are spaced 211 mm apart [153].

the spectral dependence $E_{ab}(\nu)$, because the energy absorbed at the wings of the SF_6 MPA spectrum is low and insufficient to maintain cluster disintegration (Fig. 21). The width of the dependence $E_{res}(\nu)$ decreases sharply with decreasing excitation energy density. For example, the width of the spectral dependence $E_{res}(\nu)$ measured by us at $\Phi \approx 0.5$ J cm^{-2} was roughly 6 cm^{-1} (at half height), and that of $E_{res}(\nu)$ less than 4 cm^{-1}.

The results of Refs [152, 153] and available literature data on the IR MPA of SF_6 beam molecules were utilized to estimate the size of the clusters that disintegrated in collisions with vibrationally excited molecules. It turned out, for example, that trapping of a single SF_6 molecule vibrationally

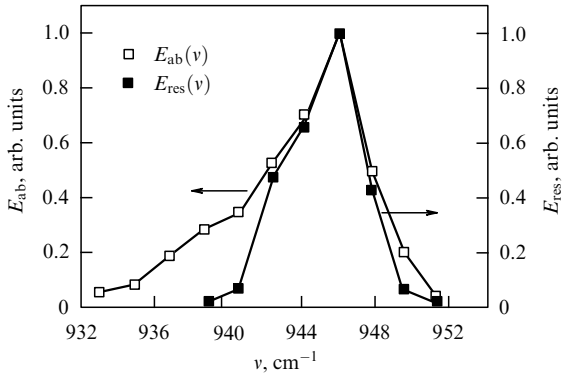

Figure 21. Frequency dependences of SF_6-absorbed energy in the beam E_{ab} (white squares) and residual (following cluster disintegration) energy E_{res} in SF_6 molecules (black squares). Energy density of SF_6-exciting CO_2-laser radiation was 1.1 J cm^{-2} for the dependence $E_{ab}(\nu)$, and 1.0 J cm^{-2} for the dependence $E_{res}(\nu)$. Other experimental conditions are the same as in Fig. 20 [152, 153].

excited at the laser 10P(16) line (947.74 cm^{-1}) and energy density $\Phi \approx 0.6$ J cm^{-2} completely disintegrated an argon cluster with up to $N \approx 20$ atoms. If each cluster trapped (with a high probability due to the use of a rather high-intensity beam) two excited molecules from the intersecting molecular beam, argon clusters with up to about $N \approx 30-40$ atoms underwent disintegration. In most experiments conducted in Refs [152, 153], more than one SF_6 molecule was trapped by a cluster, because the deflection angle of the cluster beam ($\theta \approx 10^\circ$) was consistent with the trapping of just two SF_6 molecules by each argon cluster containing $N \approx 30$ atoms. The actual trapping of more than one SF_6 molecule by clusters was experimentally confirmed in paper [153].

The $E_{res}(\Phi)$ dependences, analogous to those obtained with argon clusters, were observed in Ref. [153] describing the interaction of vibrationally excited SF_6 molecules with $(N_2)_N$ and Kr_N van der Waals clusters characterized by low atomic and molecular binding energies. Specific sublimation energies of particles on the surface of macroscopic substances N_2 and Kr were roughly 0.07 and 0.116 eV [166, 167]. It was shown in paper [153] that Xe_N clusters also underwent fragmentation despite their much higher atomic binding energy (the particles' sublimation energy was around 0.164 eV) [166, 167]. The results of Ref. [153] confirmed the general character of disintegration of weakly bound van der Waals clusters colliding with highly vibrationally excited molecules. Moreover, it was shown in Ref. [153] that the higher the binding energy of atoms (molecules) in the clusters, the higher the energy of SF_6 molecules colliding with them, at which they begin to fragment.

Thus, it was demonstrated in Refs [152, 153] that during collisions between SF_6 molecules highly vibrationally excited by IR laser radiation (with the vibrational energy $E_{vib} \geqslant 0.5$–2.0 J cm^{-2}) and Ar_N, Kr_N, and $(N_2)_N$ ($N \leqslant 30-40$) clusters in intersecting molecular and cluster beams, the clusters trap the molecules and thereafter undergo complete disintegration with the release of the captured molecules. Cluster disintegration is highly sensitive to the vibrational energy of captured molecules, i.e., to their IR absorption spectrum (Fig. 21). This explains why only excited molecules induce disintegration of the clusters that trapped them.

Unexcited SF_6 molecules trapped by clusters cause a few atoms to evaporate from their surface (by transferring kinetic

energy to the clusters) and are taken away by the cluster beam, whereas the SF_6 molecules released after cluster disintegration in the laboratory reference frame have a wider directional diagram than cluster beams. This fact is attributable to the large number of recoil episodes experienced by a cluster during atom evaporation. For this reason, the method in question, as well as the method for selective molecule trapping by clusters described in Section 8.1, can be applied to separate isotopes by laser irradiation. At the same time, the efficiency of the methods considered in Sections 8.1 and 8.2 is rather low, and they are rather difficult to employ in practice.

9. SILEX company and its technology

9.1 SILEX company

As is known from publicly available information [171–177], the Separation of Isotopes by Laser EXcitation company (SILEX Ltd. or SSL) was set up by Michael Goldsworthy for technological research and development in Australia in 1988. In 1990, SSL initiated isotope separation studies under the guidance of Horst Struve. In 1993, it formulated the fundamentals of laser-assisted isotope separation, described as unique by the developers. In 1995, a laboratory affiliated with the company and located in the southern outskirts of Sydney in a small town of Lukas Heights elaborated the evidence-based principles of the SILEX process. The company focused on isotope separation for uranium enrichment, which makes up the most important segment of the global isotope market.

In 1999, the governments of the USA and Australia signed an agreement of cooperation for the further development of SILEX uranium enrichment technology to be subsequently transferred to the USA. The macroscopic process of uranium enrichment was for the first time successfully demonstrated in 2000 [172]. The SILEX technology has been kept secret by US and Australian authorities since 2001. An important step in the SILEX-based uranium enrichment project was accomplished in 2002: the developers performed uranium enrichment under practical conditions. In 2004, the SILEX company put into operation the world's first experimental facility for laser-assisted silicon enrichment. In 2006, SSL and General Electric signed a license agreement on uranium enrichment using SILEX technology [171, 172, 176, 178]. In the same year, it was approved by the US government.

In the first half of 2007, the SILEX project was transferred to a General Electric nuclear fuel plant based in Wilmington, NC, USA. Hitachi and Cameco (the world's largest uranium producer) joined General Electric as part owners of the Global Laser Enrichment (GLE) business venture comprising General Electric (51%), Hitachi (25%), and Cameco (24%) and began to construct a pilot facility for laser enrichment of uranium in Wilmington. The US Nuclear Regulatory Commission (NRC) approved the GLE license for the development of the test cycle of uranium enrichment by SILEX technology in 2008 [179–182].

In July 2009, GLE announced the initiation of a test cycle for the assessment of the SILEX technology. In the same year, GLE applied to the NRC for the license to set up a commercial enterprise in Wilmington. In April 2011, GLE and SSL reported successful completion of measurements in the framework of the first test cycle [171, 172]. In 2012, NRC approved the GLE application for establishing the commercial venture for SILEX-based uranium enrichment. GLE invests US$500 mln to building and commissioning of the Wilmington pilot plant to evaluate prospects for industrial-scale uranium enrichment [171, 172]. The first phase of the test cycle was completed in Wilmington in May 2013. The operability of the SILEX technology has been confirmed and successfully demonstrated [171].

It is also expected in Refs [171, 172] that GLE will construct one more SILEX-based uranium enrichment facility instead of the plant for isotope separation by diffusion technology in Padukah, KY, USA, after its planned shutdown. The primary objective of this project consists in commercial uranium tail processing (estimated reserves are a few hundred thousand tons) to enrich U-235 depleted uranium either to the natural isotope composition or to an industrially relevant level. In 2014, the US Department of Energy (DOE) chose GLE to run this enterprise. Contract negotiations between the DOE and GLE on the use of the SILEX technology for re-enrichment of the depleted uranium tailings over the next 40 years are in progress [171, 172].

9.2 SILEX technology

It is the opinion of the project's developers that SILEX technology has a number of advantage over other methods of uranium enrichment [171]: (1) a much higher effectiveness of the enrichment process, (2) lower operating costs, and (3) significantly smaller capital expenditures than with centrifugation technologies. And what is of paramount importance, the SILEX technology is currently the only actively developing technology of laser–assisted uranium enrichment. It is expected in Ref. [171] that the third-generation SILEX technology will replace the old methods, such as gas diffusion and gas centrifugation (first- and second-generation technologies, respectively), providing actually the most effective approach to solving the nuclear fuel problem.

According to SSL [171, 183], enrichment efficiency using the SILEX technology is much higher (1.6–16 times) than that of centrifugation. It consumes less power and needs smaller areas to operate in. Advocates of the SILEX technology [171, 183] believe that this less expensive and more efficacious method of uranium enrichment will be instrumental in reducing the costs of energy production and turning nuclear power engineering into a competitive industry.

Details of SILEX technology are kept carefully under wraps. However, some of them can be deduced from the analysis of publicly available open information [171, 183] and the known methods of laser-based uranium enrichment (AVLIS, MLIS, by IR MPD of UF_6 molecules). To recall, the AVLIS technique is based on selective ionization of uranium atoms in the vaporized state [8, 9, 184]. Their ionization energy is roughly 6.2 eV [166]. The uranium atomic vapor is produced by evaporating metallic uranium with an electron beam. Frequency-tuned copper-laser-pumped dye lasers or diode lasers are used for the ion production. Atomic ionization is usually a three (or two)-step process. Lasers operating at different wavelengths are employed at each step. They are tuned to be in close resonance with electron transitions in the ^{235}U isotope. The resulting $^{235}U^+$ ions are picked up into a negatively charged collector. The starting matter and its processing products have the same chemical composition.

MLIS is based on isotope-selective dissociation of UF_6 molecules by selective vibrational IR laser excitation. Further dissociation is accomplished either by the same IR laser or by

a ultraviolet (UV) laser [7, 10, 11, 184]. Molecules are excited and dissociated in a gas-dynamically cooled molecular flux. The energy needed to maintain these processes ranges 3.5–4.5 eV. The starting material and its derivatives have a different chemical composition. UF_6 dissociates into UF_5 and F. In this process, the UF_6 gas is mixed with a proper carrier gas (usually an inert gas) and an acceptor of fluorine atoms (most frequently methane or hydrogen). Frequency-tunable laser radiation at a 16-μm wavelength resonant with ν_3 vibrational mode of $^{235}UF_6$ molecules is used for their selective vibrational excitation. $^{235}UF_5$-rich solid particles resulting from molecule dissociation are deposited on collector riffled plates [184].

The SILEX technology also employs UF_6 molecules as the starting material, mixed with a carrier gas in a gas-dynamic flow. As is known from Ref. [173], all three main flows in this process, viz. the initial gas, processing products, and residual gas, are composed of UF_6 molecules, which means that the method takes advantage of intermolecular forces instead of molecule dissociation (paper [173] also elucidates some other characteristics of the process).

First, the molecule excitation mechanism is analogous to that in MLIS technology based on molecular dissociation, and reduces to enhancing the vibrational energy of the molecules. Some authors believe that the SILEX technology is underlain by laser-induced inhibition of clusterization during gas-dynamic cooling of the gas at the nozzle exit [11] (see Section 4).

Second, promoters and advertisers of the SILEX technology maintain that it requires much lower energy than MLIS based on molecular dissociation. In other words, it is less expensive than centrifugation technologies [185]. It appears that the former method will employ either isotope-selective suppression of clusterization of UF_6 molecules (see Section 4.2) or isotope-selective dissociation of dimers or small clusters of UF_6 molecules alone or mixed with the carrier gas (see Section 3.2). Probably, a combination of these two approaches (see Section 4.2) will be implemented.

It follows from Refs [171, 177, 183, 186] that the SILEX process includes irradiation of a gas-dynamically cooled flow of UF_6 molecules mixed with a carrier gas by a tunable pulsed laser operating at a 16-μm wavelength resonant with ν_3 vibrational mode of UF_6 molecules. Emission at this wavelength is generated by forced Raman scattering of pulsed CO_2-laser radiation with a wavelength of 10.6 μm in parahydrogen. Also, a tunable 16-μm diode laser can be employed. The 16 μm laser selectively excites first and foremost $^{235}UF_6$ molecules, thereby creating a difference between the ratios of isotopomers in the product flow enriched with ^{235}U and in the residual gas flow dominated by ^{238}U (see Sections 3 and 4). The SILEX technology can be applied to enrich chlorine, molybdenum, and uranium isotopes; analogous technologies are also suitable for carbon and silicon enrichment [171].

10. Selective infrared multiphoton dissociation of molecules under nonequilibrium conditions of a pressure shock as an alternative to low-energy methods of molecular laser isotope separation

References [187–194] deal with the selective IR MPD of SF_6 and CF_3I molecules in gas-dynamically cooled pulsed molecular flows interacting with a solid surface, including those formed under pressure shock (wave) conditions. It is the author's opinion that the proposed approach (see also review [123]) may become a promising alternative to the low-energy methods of molecular laser isotope separation, the development of which is currently underway. The above work demonstrates that excitation of molecules under nonequilibrium conditions of a pressure shock in front of the surface ensures high product yield and selectivity at a relatively low energy density (below about 1.5–2 J cm^{-2}). These values are 3–5 times smaller than energy densities needed for molecule dissociation in unperturbed jets and flows, implying the possibility of isotope separation at relatively low laser radiation energy densities.

Thus, the approach developed in Refs [187–194] and based on molecular dissociation process can be regarded, due to the moderate energy density needed to maintain it, as an alternative to low-energy methods of molecular laser isotope separation. The principles of this approach and certain results obtained with its help are briefly considered in Sections 10.1–10.6.

10.1 Nonequilibrium conditions in a pressure shock

Isotope-selective dissociation of molecules characterized by small isotope shifts in IR absorption spectra is usually proceeded in gas-dynamically cooled jets and flows [7, 123]. During molecular gas outflow from the nozzle, all degrees of freedom of a molecule reside initially in thermodynamic equilibrium. As the gas cools rapidly due to expansion, the thermodynamic equilibrium between different degrees of freedom becomes upset, because the translational, rotational, and vibrational relaxation times differ: $\tau_{tr} \leqslant \tau_{rot} \leqslant \tau_{vib}$. The degree of departure from local equilibrium depends on the number of collisions z_{col} necessary for relaxation of a given degree of freedom. Generally, the condition $z_{tr} \leqslant z_{rot} \leqslant z_{vib}$ is fulfilled for polyatomic molecules. Therefore, the condition

$$T_{1,tr} \leqslant T_{1,rot} \leqslant T_{1,vib} \tag{10.1}$$

is realized for effective temperatures in the flow [195].

Nonequilibrium conditions that are inverse relative to inequality (10.1) can be realized in the shock wave [196–198] formed by a gas-dynamically cooled molecular flow impacting a solid surface due to the difference among translational, rotational, and vibrational relaxation rates. Thus, one finds

$$T_{2,tr} \geqslant T_{2,rot} \geqslant T_{2,vib}\,. \tag{10.2}$$

Because vibrational–translational relaxation takes much time (e.g., rate constant $p\tau_{V-T} \approx 150$ μs Torr for SF_6 molecules [200], and $p\tau_{V-T} \approx (350 \pm 100)$ μs Torr for CF_3I [201]), the vibrational temperature of the molecules in the shock wave formed in a pulsed rarefied gas flow may be virtually equal to that in the incident gas flow ($T_{2,vib} \approx T_{1,vib}$). At the same time, translational and rotational temperatures of the molecules in a pressure shock are much higher than in the incident flow: $T_{2,tr} > T_{1,tr}$ and $T_{2,rot} > T_{1,rot}$.

In other words, new nonequilibrium conditions created in the pressure shock are characterized by a significantly lower vibrational temperature of the molecules compared with the translational and rotational temperatures. It is under such conditions that the selective dissociation of SF_6 and CF_3I molecules was investigated in Refs [187–194].

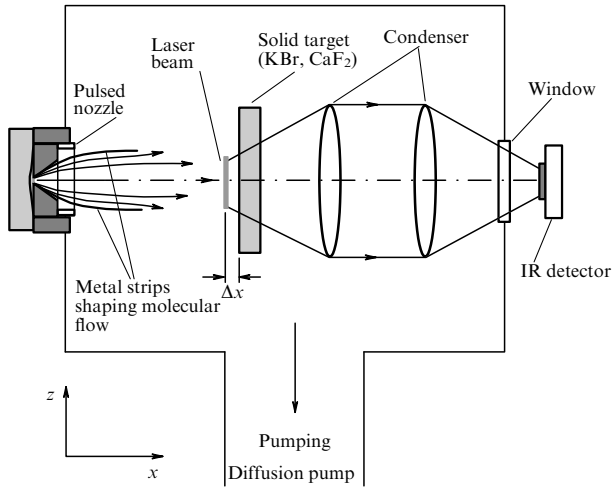

Figure 22. Schematic diagram of the experimental setup (cross section in the *xy* plane; the laser beam is directed along the *y*-axis) [187, 190].

10.2 Experiment and research method

10.2.1 Experimental setup. Figure 22 depicts a schematic diagram of the experimental setup. The flow of molecules was formed in a 'current loop' type pulsed nozzle [133]. The nozzle orifice diameter was 0.75 mm, and the nozzle-opening pulse duration (at half height) was 100 μs. The gas pressure above the nozzle could be varied in a range from 0.1 to 3.5 atm. The nozzle outlet orifice had a cone shape with a vertex angle of 60° and a height of 15 mm. The total number of molecules $N_{\rm fl}$ in the flow emitted from the nozzle per pulse depended on the above-nozzle gas pressure. In the experiment of interest, N was varied from 5×10^{15} to 1.5×10^{17} molecules per pulse [190, 192]. The nozzle could operate both in the regime of single pulses and in the repeated pulse mode with a pulse repetition rate of up to 1 Hz. The molecular flow was formed in a vacuum chamber (with the volume of $V_{\rm ch}$ being 20 l) evacuated to a pressure of $(1-2) \times 10^{-6}$ Torr. The molecular flow was formed with the aid of two thin metal strips fixed at the nozzle outlet cone so as to form a dihedral angle with the edge parallel to the *y*-axis, and a variable radius of curvature in the *xz* plane.

Spaced $x = 50 - 150$ mm apart the nozzle, a solid target (plates made from KBr, CaF_2, or LiF crystals, which were transparent to HF^* luminescence) was placed behind the nozzle and oriented so that the surface was perpendicular to the gas flow. The interaction of the pulsed supersonic molecular flow with the solid surface led to the formation of a shock wave in front of the surface [196–198] with essentially inhomogeneous, nonstationary, and nonequilibrium conditions established in this region. Under the present experimental conditions, the characteristic size of the shock wave front was 0.2–5 mm [190–192], i.e., of the same order of magnitude as the mean free path of molecules [196, 197].

The molecules were excited by radiation from a tunable high-power CO_2 laser with a total pulse energy of up to 3 J. The molecules were excited at the distance $\Delta x = 1.5-8.0$ mm from the solid surface. The laser radiation was focused onto this region with the aid of a cylindrical lens with a focal length of 12 cm. The lens axis was parallel to the solid surface. The laser beam cross section at the focal spot was about 0.18×12.5 mm^2. The nozzle, the CO_2 laser, and the lock-in registration system including an HF^* luminescence detector (or a pyroelectric detector with an amplifier) and an S9-8 digital oscillograph were triggered by a delay pulse generator built around a GI-1 oscillator. The synchronism between the laser pulses and the pulsed molecular flow was monitored with the aid of the pyroelectric detector measuring a signal induced by vibrationally excited molecules [135, 136] or by measuring the HF^* luminescence signal.

10.2.2 Research method. The dissociation of SF_6 molecules in a gas flow was studied by detecting luminescence from HF^* molecules ($\lambda \approx 2.5$ μm). The vibrationally excited HF^* molecules were produced in the reactions between fluorine atoms (the primary product of the dissociation of the SF_6 molecule) and hydrogen or methane [202]. The HF^* luminescence intensity was well correlated with the SF_6 dissociation yield [203, 204]. The luminescence was measured using a PbS-based IR detector with a working sensor area of 1×1 cm^2.

Also measured was the yield of SF_4 product and the coefficient of its enrichment with isotope ^{34}S. A procedure employed for collecting the dissociation products and for the IR analysis of these products and the gas being retained after its irradiation during molecular dissociation in the gas-dynamic flow was described at length in Refs [134, 163]. The coefficient of the SF_4 enrichment with the ^{34}S isotope was defined as

$$K_{34}^{\rm prod} = \frac{[^{34}{\rm SF}_4]}{[^{32}{\rm SF}_4]} \frac{1}{\xi}\,, \tag{10.3}$$

where $[^{34}SF_4]/[^{32}SF_4]$ is the ratio of the concentrations of molecules indicated in square brackets in the SF_4 product, $\xi = {}^{34}{\rm S}/{}^{32}{\rm S} \approx 0.044$ is the sulfur isotope ratio in the initial SF_6 gas. The ratio of the concentrations of $^{34}SF_4$ and $^{32}SF_4$ molecules in the product was determined from IR absorption spectra measured in the region of ν_6 vibrational mode of the molecule (≈ 728 cm^{-1} for $^{32}SF_4$ [205]), for which the isotope shift between $^{32}SF_4$ and $^{34}SF_4$ was approximately 12.3 cm^{-1} [206].

In experiments with a CF_3I molecule, the yield of the C_2F_6 product and the coefficient of its enrichment with the isotope ^{13}C were measured. The measurements were made based on the analysis of the IR and mass spectra of the products and the residual gas. The isotope composition of C_2F_6 was determined from the $C_2F_5^+$ ion fragment. The coefficient of C_2F_6 enrichment was found from the relation

$$K_{13}^{\rm prod} = \frac{2I_{121} + I_{120}}{(I_{120} + 2I_{119})\,\xi}\,, \tag{10.4}$$

where I_{119}, I_{120}, and I_{121} are the intensities of $C_2F_5^+$ ion mass-peaks, and $\xi = {}^{13}{\rm C}/{}^{12}{\rm C} \approx 0.011$ is the ratio of the percent compositions of carbon isotopes in the starting CF_3I gas.

10.3 Spectral and energy characteristics of molecular dissociation

The spectral and energy characteristics of SF_6 and CF_3I dissociation in the case of their excitation under the nonequilibrium conditions of a pulsed flow interacting with a solid surface were considered in Refs [188, 190, 192] and [191], respectively. It was shown that the intensity of HF^* luminescence in a wide range of energy densities for SF_6 excitation in a pressure shock or in a flow incident on the surface is much higher than for molecular excitation in an unperturbed flow (Fig. 23a). HF^* luminescence intensity in the flow incident on the surface and in the pressure shock was roughly 3–4 and

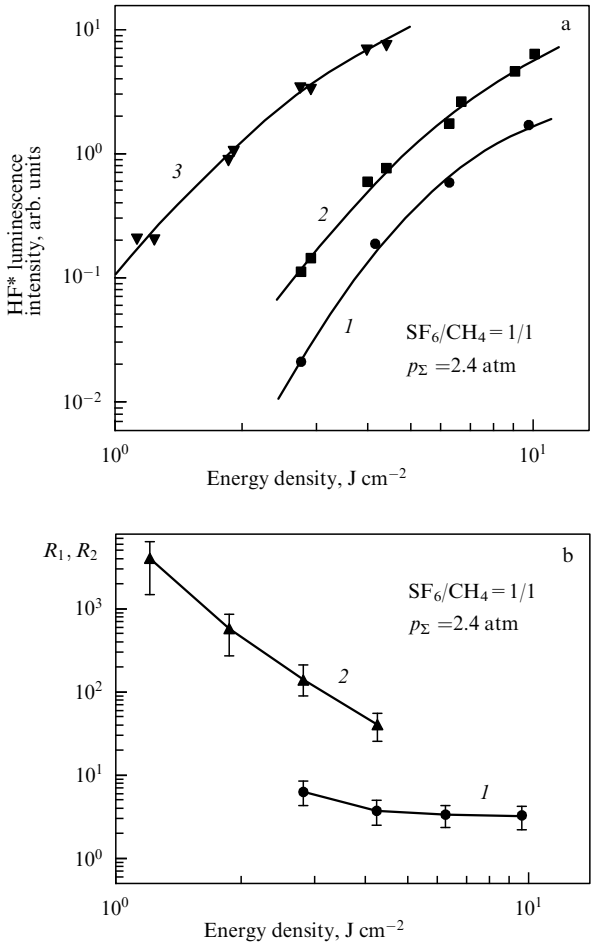

Figure 23. (a) Plots of HF* luminescence intensity versus excitation energy density for SF_6 molecules excited in the presence of CH_4 molecules ($p_{SF_6}/p_{CH_4} = 1/1$) in an unperturbed flow (curve *1*), in a flow incident on a solid surface (curve *2*), and in a shock wave (curve *3*). Total gas pressure above the nozzle $p_\Sigma = 2.4$ atm; nozzle-to-target surface distance (for curves *2* and *3*) $x = 51$ mm; $\Delta x = 2.5$ mm; excitation frequency was 945.98 cm^{-1} (laser line 10P(18)) [190, 192]. (b) Dependences of R_1 and R_2 ratios of HF* luminescence intensities in the flow incident on the surface (curve *1*) and in the shock wave (curve *2*) to HF* luminescence intensity in an unperturbed flow on the energy density of laser exciting radiation (based on the data of Ref. [190]).

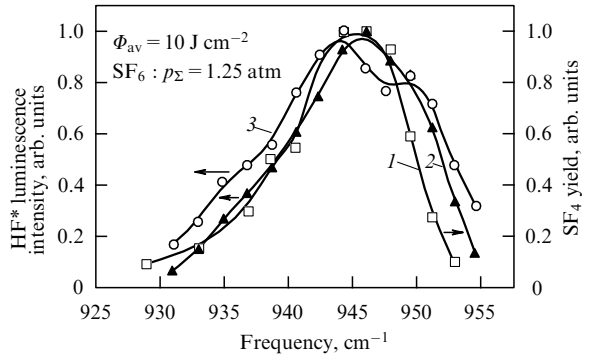

Figure 24. Plots of HF* luminescence intensity versus laser radiation frequency for SF_6 molecules excited in a flow incident on a solid surface (curve 2*)* and in a shock wave (curve *3*). Total SF_6 pressure above the nozzle is $p = 1.25$ atm; nozzle-to-target surface distance $x = 51$ mm; $\Delta x = 2.5$ mm. Averaged energy density amounts to 10 J cm^{-2} [190]. For comparison, curve *1* shows the frequency dependence of the SF_4 product yield obtained in Ref. [207].

more than 30 times higher, respectively, than in an unperturbed flow. The difference is even greater at excitation energy densities $\leqslant 3$ J cm^{-2} (Fig. 23b). This suggests a substantial contribution from collisional dissociation of the molecules in the shock wave to the total dissociation yield at small energy densities.

These results imply that molecule excitation in the shock wave and in the flow incident on the surface leads to a greater yield of the dissociation products than in the case of excitation in the unperturbed flow. Therefore, it would be of interest to study a selectivity of the dissociation process in the flow interacting with the solid surface. Such a study was carried out in Refs [188, 190–193]. The dependences of HF* luminescence intensity on the frequency of laser exciting radiation (i.e., the spectral dependences of the dissociation yield) in the case of SF_6 excitation were considered in Refs [188, 190, 192, 193], and the spectral dependences of the C_2F_6 product yield in the case of CF_3I excitation in Ref. [191].

Figure 24 displays the spectral dependences of HF* luminescence intensity for SF_6 excitation in a flow incident on a solid surface (curve *2*), and in a shock wave (curve *3*). For comparison, the figure shows the frequency dependence of the SF_4 product yield (curve *1*) obtained previously [207] for SF_6 excited in a molecular flow under experimental conditions identical to those in Refs [190, 192]. Curve *1* can be considered as the spectral dependence of the SF_6 dissociation yield in the unperturbed flow. The spectra are normalized to the maximum intensities. Although *2* and *3* spectra are wider than *1*, the ratios of intensities in the maxima and low-frequency wings (near the absorption band corresponding to vibrational mode ν_3 in $^{34}SF_6$ (≈ 930.5 cm^{-1}) [148]) are not significantly different for all of them. This indicates that the selectivities of dissociation in these cases are not significantly different as well, which was confirmed by measurements of process selectivity.

It was also revealed in Refs [190, 193] that the spectral dependences of the SF_6 dissociation yield in the case of molecule excitation in the pressure shock are much narrower than for excitation in a cell at room temperature, because the vibrational temperature of molecules in the shock wave is much lower than room temperature.

It was established in Ref. [191] that the yield of C_2F_6 for CF_3I excitation in the pressure shock is much higher at all frequencies than for excitation in an unperturbed flow (Fig. 25). In the former case, the yield of C_2F_6 product in the maximum (lines 9R(10) and 9R(12)) was 12–15 times higher; it was more than 200 times higher in the low-frequency wing (e.g., at the 9P(20) line coincident with the $^{13}CF_3I$ absorption band). Such a striking difference between C_2F_6 yields in molecule excitation at the far wing of the spectrum is largely due to the strong dependence of the product yield on the concentration of the irradiated molecules [134, 208, 209] attributable to the formation of the C_2F_6 product in pair collisions of CF_3 radicals. Another cause for this discrepancy is related to the rather high rotational temperature of CF_3I molecules in the shock wave compared with that in an unperturbed flow [191].

It was also shown in Refs [190, 192] that molecule dissociation yield markedly increases as distance Δx between the target surface and the excitation zone decreases. The spectral dependences of the dissociation yield at different Δx have been studied in Refs [193, 194]. The spectral dependences of HF* luminescence intensity for $\Delta x \geqslant 2.5$ mm are

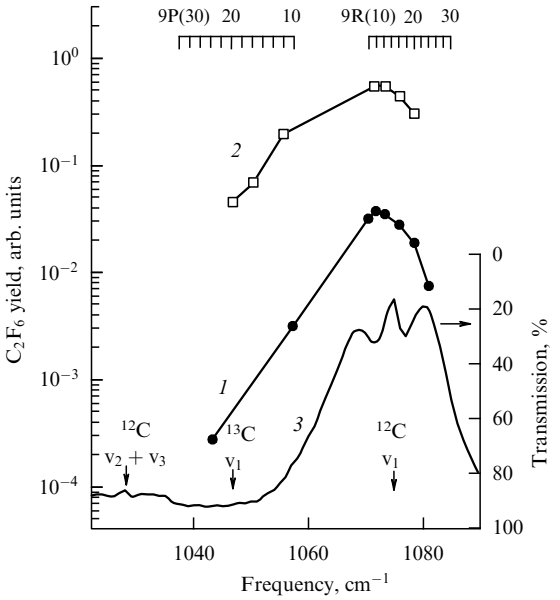

Figure 25. Plots of C_2F_6 yield versus laser radiation frequency for CF_3I molecules excited in an unperturbed flow (curve *1*) and in a shock wave (curve *2*). Nozzle-to-target surface distance $x = 51$ mm; $\Delta x = 2.5$ mm. Molecules were excited at the laser line 9R(12) at an energy density of 1.4 J cm^{-2}. Total gas pressure above the nozzle is 1.5 atm. Curve *3* corresponds to the CF_3I linear absorption spectrum. CO_2-laser generation lines are shown at the top [191].

practically the same in width as analogous dependences in an unperturbed flow, which implies that the selectivity of dissociation of $^{34}SF_6$ molecules in all these cases should not be substantially different, as confirmed in Refs [188, 190, 192]. At small distances $\Delta x \leqslant 1.5$ mm, when molecules are excited rather close to the surface, the low-frequency wing of the spectral dependence is more intense than in the unperturbed flow, which implies worse selectivity of molecular dissociation. Nevertheless, the spectral dependences observed remain significantly narrower than the analogous dependences at room temperature.

10.4 Product yield and selectivity of the process

Direct measurements of the yield of the end products (SF_4 and C_2F_6) and selectivity upon SF_6 and CF_3I excitation in a flow interacting with the surface and in an unperturbed flow were made in Refs [188, 190, 192] and [191], respectively. The measuring method has been described earlier [163, 207, 208]. It was shown that the excitation of molecules in a flow incident on the surface and in a shock wave ensured a yield of SF_4 molecules of 2.5 and over 12 times that in an unperturbed flow, respectively.

The selectivity of the process was evaluated by measuring the enrichment coefficients of SF_4 and C_2F_6 products with ^{34}S and ^{13}C isotopes in SF_6 or CF_3I molecule excitation in the incident flow interacting with a solid surface, pressure shock wave, and unperturbed flow. SF_6 molecules were excited at a frequency of 929 cm^{-1} (CO_2-laser line 10P(36)) in resonance with a vibrational mode ν_3 of $^{34}SF_6$ [148]. CF_3I molecules were excited at the CO_2-laser line 9P(20) with a frequency of 1046.85 cm^{-1} in close resonance with vibrational mode ν_1 of $^{13}CF_3I$ [139]. The results of measurements are presented in Tables 2 and 3 together with the product yield information. The enrichment coefficients K_{34}^{prod} were 17 ± 5 and 14 ± 3 for SF_6 excitation at an energy density of 10 J cm^{-2} in the unperturbed flow and in the pressure shock, respectively. They were $K_{13}^{\text{prod}} = 21 \pm 3$ and 15 ± 3, when CF_3I molecules were excited in the unperturbed flow and in the pressure shock, respectively, meaning that selectivity of molecule dissociation in the pressure shock is only slightly worse (roughly 25–30%) than in the unperturbed flow, while the product yield in the pressure shock is ten times higher.

A rise in the product yield in the case of molecule excitation in the pressure shock is a result of increasing temperature, gas density, and molecule dissociation yield. A rise in the molecule dissociation yield occurs, in turn, due first to the higher efficiency of molecular excitation in the pressure shock, and second to collisional dissociation of molecules whose energy does not reach the dissociation threshold level after excitation by an IR pulse (such molecules fail to dissociate in unperturbed flows because of the deficit of collisions) [190, 192]. The relatively high dissociation selectivity in the pressure shock is a consequence of stably low

Table 2. Yield of SF_4 product and coefficient of its enrichment with ^{34}S isotope for SF_6 excitation in an unperturbed flow, a flow incident on the surface, and in a shock wave at a pressure of SF_6 of 1.25 atm above the nozzle [190].

CO_2-laser line	Energy density, J cm^{-2}	Yield of SF_4 product, arbitrary units			Enrichment coefficient, K_{34}^{prod}		
		Unperturbed flow	Flow incident on surface	Shock wave	Unperturbed flow	Flow incident on surface	Shock wave
10P(16)	12	1.0 ± 0.2	2.5 ± 0.5	12 ± 3	—	—	—
10P(36)	10	—	—	—	17 ± 5	15 ± 3	14 ± 3

Table 3. Yield of C_2F_6 product and coefficient of its enrichment with ^{13}C isotope for CF_3I excitation in an unperturbed flow, a flow incident on the surface, and in a shock wave at a pressure of CF_3I of 1.5 atm above the nozzle [191].

CO_2-laser line	Energy density, J cm^{-2}	Yield of C_2F_6 product, arbitrary units			Enrichment coefficient, K_{13}^{prod}		
		Unperturbed flow	Flow incident on surface	Shock wave	Unperturbed flow	Flow incident on surface	Shock wave
9R(12)	1.3	1.0 ± 0.2	2.5 ± 0.5	14 ± 3	—	—	—
9P(20)	1.5	—	—	—	21 ± 3	19 ± 3	15 ± 3

vibrational temperature. It was established in Ref. [193] that the vibrational rather than rotational temperature of molecules is the main factor responsible for setting the degree of selectivity.

10.5 Assessment of the efficiency of the method

The results of research [190, 192] make it possible to assess the efficiency of the method of molecule dissociation in a pressure shock, as exemplified by SF_6 dissociation and the formation of enriched $^{34}SF_4$ product using the experimental setup described in a preceding section and the measured parameters of the molecular flow [190]. For example, as many as $N_{fl} \approx 6 \times 10^{16}$ SF_6 molecules left the nozzle per pulse when the pressure above the nozzle was $p_{SF_6} = 2$ atm. The flow volume was $V_{fl} \approx 30$ cm^3, and the average molecule concentration in the flow was $N_1 \approx 2 \times 10^{15}$ cm^{-3}. The mean concentration of SF_6 molecules in the shock wave was $N_2 \approx 2.8 \times 10^{16}$ cm^{-3} [123, 190]. The size of the shock wave front for SF_6 ranged approximately 3 mm. Laser radiation with moderate energy density allowed irradiating a volume of gas determined by the geometric cross section (e.g., 1.5 mm $\times$ 20 mm) of the focused laser beam and the length of the irradiated zone along the target surface ($\approx$ 10 cm), i.e., $V_{exc} \approx 3$ cm^3.

$^{34}SF_6$ molecules are known to account for 4.2% of the isotopomers in their natural mixture. The concentration of $^{34}SF_6$ molecules in the irradiated volume was $\approx 1.2 \times 10^{15}$ cm^{-3}, and the total number of molecules $\approx 3.6 \times 10^{15}$. At the laser radiation energy density $\Phi \approx 1.5$ J cm^{-2}, the molecule dissociation yield in a shock wave was $\beta \approx 0.3$, as follows from the fact that the signal of HF^* luminescence in the pressure shock corresponded to that in the unexcited molecular flow at the excitation energy density $\Phi \approx 6.5-7.0$ J cm^{-2} (Fig. 23a), when the dissociation yield of SF_6 molecules was $\beta \geqslant 0.3$ [138]. This means that the number of $^{34}SF_6$ molecules that underwent dissociation per pulse was $\approx 1.1 \times 10^{15}$. If the pulse repetition rate is 100 Hz, the yield of $^{34}SF_4$ molecules per hour without regard for the losses in chemical reactions may be as high as $\approx 4 \times 10^{20}$ or $\approx 10^{22}$ molecules per day, which corresponds to approximately 1.6×10^{-2} mol (roughly 1.8 g/day). These values are significantly higher (by two orders of magnitude) than the analogous estimates for the case of $^{10}BCl_3$ enrichment by selective vibrational predissociation of $Ar-^{10}BCl_3$ clusters (see Section 3.2). They are roughly four orders of magnitude higher than in $^{34}SF_6$ enrichment with the use of helium nanodroplets (see Section 6.3) and almost one and a half or two orders of magnitude higher than obtained in the IR MPD of UF_6 molecules (see Section 6.4).

It is worthwhile to note that a CO_2 laser with a pulse energy below 0.7–1.0 J must be used to carry out such a process. Under these conditions, no more than 1.5–2.5% of the laser energy is absorbed due to the relatively high dissociation selectivity (about 14 in the case of SF_6 molecules; see Table 2). A vacuum of $(0.5-1) \times 10^{-3}$ Torr will be sufficient for this purpose. Therefore, the isotope separation process may be scaled up, e.g., by using a series of circular or slotted pulsed nozzles.

10.6 Summary

References [187–194] gave evidence that the excitation of molecules in flows incident on a surface causes a substantial increase (several-fold) in the product yield compared with that resulting from their excitation in unperturbed flows, without an appreciable decrease in the selectivity of the process. Excitation in a pressure shock increases the product yield by more than ten times over that in unperturbed flows, with a slight loss (25–30%) of the process selectivity. In other words, the formation of a shock wave in front of a solid surface permits significantly improving the effectiveness of selective multiphoton IR dissociation of molecules in pulsed gas-dynamically cooled molecular flows.

To conclude this section, it is worthwhile to emphasize the advantages of this method over low-energy techniques for laser isotope separation considered in the preceding sections. The main advantages consist in the high efficiency of isotope separation and technical simplicity, as demonstrated in experiments [187–194] describing conditions for enhanced product yield without detriment to selectivity. Both the product yield and selectivity were measured experimentally in enriched gas actually produced and collected in a cell, in contrast to the online mass-spectrometric detection in many other techniques.

Moreover, the above studies demonstrate the advantages of the method in question over the IR MPD of molecules in unperturbed jets and flows. Therefore, the isotope-selective IR MPD of molecules under the nonequilibrium conditions of a pressure shock can be regarded as a promising alternative to low-energy methods of molecular laser isotope separation.

11. Conclusions

The results considered in Sections 2–9 provided a basis for several approaches to IR laser-induced isotope-selective processes proceeding at relatively low molecule activation energies ($\leqslant 1$ eV). Some of them are still poorly known and rarely employed. They include molecule selection by low-energy electron attachment and by using clusters and nanoparticles. Others are inefficient and/or difficult to apply for practical implementation. Nonetheless, certain methods have good prospects for the development of low-energy techniques of molecular laser isotope separation.

Isotope separation by technologies based on low-energy electron attachment or the employment of superfluid helium nanodroplets, clusters, and nanoparticles is an inefficient process. Specifically, the first method is characterized by small cross sections of dissociative electron attachment, compared with the capture cross sections in the formation of negative molecular ions, while the other two methods employ low concentrations of the starting material highly diluted with the carrier gas (in clusters). Moreover, these techniques are difficult to realize under practical conditions. Their comparison in terms of efficiency based on objective criteria is equally irrelevant in view of the lack of experimental data concerning the main parameters of the separation process, e.g., selectivity, product yield, and irradiation geometry.

It is worthy of note in this context that the efficiency of SILEX (assuming it to be a well-developed technology) in comparison with the centrifugation technique [171, 183] is estimated at 1.6 to 16, i.e. within an order of magnitude (see Section 9.2).

The methods described in Section 7 and based on the interaction of highly vibrationally excited and unexcited molecules with a cold molecule (cluster)-coated surface are more efficient than the above techniques, because they do not require strong dilution of the starting molecular gas with the carrier. Moreover, they are easier to implement under practical conditions. But the selectivity of the processes

behind these methods remains to be elucidated. Further studies are needed to this effect.

Today, the best known method of isotope separation is that of selective control of molecule clustering in gas-dynamic jets and flows with the employment of IR lasers, even though any data on its efficiency are absent. It appears to be rather low, bearing in mind that the method makes use of a molecular gas highly diluted with the carrier and that the laser irradiation zone is relatively small (within a few nozzle calibers) (see Section 4). In separating isotopes, it is possible to combine the method with IR vibrational predissociation of clusters. It can be speculated that just these methods constitute the basis of the SILEX technology.

It is the author's opinion that the isotope-selective IR MPD of molecules under nonequilibrium conditions of a pressure shock described in Section 10 can be regarded as a promising alternative to the low-energy methods of laser isotope separation considered in Sections 2–9. Although this technique is based on molecule dissociation (in this sense, it is a high-energy variant of molecular laser isotope separation), it can be regarded together with low-energy methods, taking into consideration the low energy densities needed to excite and dissociate molecules. It has been fairly well ascertained to be more efficient than the foregoing low-energy methods for molecular laser isotope separation, because it does not require strong dilution of the initial molecular gas with the carrier and is easy to realize in practice.

To conclude, of all the approaches to the implementation of IR laser-induced isotope-selective processes with low activation energy ($\leqslant 1$ eV) considered above, the approaches making use of surface heterogeneous processes (see Sections 2, 7) and those based on control of molecule clusterization and cluster dissociation (see Sections 3, 4) appear to be the most promising (from the standpoint of available information, efficiency, and possibility of practical realization) for the development of low-energy techniques of molecular laser isotope separation. An alternative to these approaches is selective IR MPD of molecules under the nonequilibrium conditions of a pressure shock wave.

Acknowledgment

The investigations presented in Sections 6–8 and 10 were conducted by the author and his co-workers of the Department of Laser Spectroscopy, Institute of Spectroscopy of the Russian Academy of Sciences. The author is profoundly grateful to V M Apatin, V N Lokhman, D D Ogurok, and A N Petin for their cooperation. The assistance of A N Petin in the preparation of drawings is also acknowledged. Thanks are due to E A Ryabov for helpful discussions and to the reviewer for valuable criticism. This study was partly supported by the Russian Foundation for Basic Research (grants Nos 12-02-00401 and 15-02-04927).

References

1. Baranov V Yu (Ed.) *Izotopy*: *Svoistva, Poluchenie, Primenenie* (Isotopes: Properties, Production, Applications) (Moscow: IzdAT, 2000)
2. Baranov V Yu et al., in *Fiziko-khimicheskie Protsessy pri Selektsii Atomov i Molekul. Sb. Dokl. 2-i Vseross. Nauchn. Konf., g. Zvenigorod, 1997* (Physical and Chemical Processes in the Selection of Atoms and Molecules. Proc. of the 2nd All-Russian Scientific Conf., Zvenigorod, 1997) (Eds V Yu Baranov, Yu A Kolesnikov) (Moscow: TsNIIatominform, 1997) p. 21
3. Letokhov V S, Ryabov E A, in *Izotopy*: *Svoistva, Poluchenie, Primenenie* (Isotopes: Properties, Production, Applications) (Ed. V Yu Baranov) (Moscow: IzdAT, 2000) p. 329
4. Baranov V Yu, Dyad'kin A P, in *Izotopy*: *Svoistva, Poluchenie, Primenenie* (Isotopes: Properties, Production, Applications) (Ed. V Yu Baranov) (Moscow: IzdAT, 2000) p. 343
5. Dyad'kin A P et al., in *Fiziko-khimicheskie Protsessy pri Selektsii Atomov i Molekul. Sb. Dokl. VIII Vseross.* (*Mezhdunarod.*) *Nauchn. Konf., Zvenigorod, 2003* (Physical and Chemical Processes in the Selection of Atoms and Molecules. Proc. of the VIII All-Russian (Intern.) Scientific Conf., Zvenigorod, 2003) (Ed. Yu A Kolesnikov) (Moscow: TsNIIatominform, 2003) p. 121
6. Letokhov V S, Ryabov E A, in *The Optics Encyclopedia*: *Basic Foundations and Practical Applications* Vol. 2 (G-L) (Eds Th G Brown et al.) (Weinheim: Wiley-VCH, 2004) pp. 1015 – 1028
7. Makarov G N *Phys. Usp.* **48** 37 (2005); *Usp. Fiz. Nauk* **175** 41 (2005)
8. Radziemski L J, Solarz R W, Paisner J A (Eds) *Laser Spectroscopy and its Applications* (Optical Engineering, Vol. 11) (New York: M. Dekker, 1987) Ch. 3
9. Bokhan P A et al. *Laser Isotope Separation in Atomic Vapor* (Berlin: Wiley-VCH, 2006)
10. Jensen R J, Judd O P, Sullivan J A *Los Alamos Sci.* **4** (1) 2 (1982)
11. Eerkens J W, Kim J *AIChE J.* **56** (9) 2331 (2010)
12. Letokhov V S *Nelineinye Selektivnye Fotoprotsessy v Atomakh i Molekulakh* (Non-Linear Selective Photoprocesses in Atoms and Molecules) (Moscow: Nauka, 1983)
13. Steinfeld J I (Ed.) *Laser-Induced Chemical Processes* (New York: Plenum Press, 1981); Translated into Russian: *Indutsiruemye Lazerom Khimicheskie Protsessy* (Moscow: Mir, 1984)
14. Bagratashvili V N et al. *Multiple Photon Infrared Laser Photophysics and Photochemistry* (Chur: Harwood Acad. Publ., 1985)
15. Molin Yu N, Panfilov V N, Petrov A P *Infrakrasnaya Fotokhimiya* (Infrared Photochemistry) (Novosibirsk: Nauka, 1985)
16. Cantrell C D (Ed.) *Multiple-Photon Excitation and Dissociation of Polyatomic Molecules* (Topics in Current Physics, Vol. 35) (Berlin: Springer-Verlag, 1986)
17. Lyman J L, in *Laser Spectroscopy and its Applications* (Optical Engineering, Vol. 11, Eds L J Radziemski, R W Solarz, J A Raisner) (New York: M. Dekker, 1987) p. 417
18. Ronander E, Strydom H J, Botha L B *Pramana J. Phys.* **82** (1) 49 (2014)
19. Klydon, http://www.klydon.co.za
20. Klydon: Applications of Isotope Separation. Uranium Enrichment, http://www.klydon.co.za/isotope_applications_uranium.html
21. Rettner C T et al. *J. Phys. Chem.* **100** 13021 (1996)
22. Miller R E *J. Phys. Chem.* **90** 3301 (1986)
23. Gurvich L V et al. *Energii Razryva Khimicheskikh Svyazei. Potentsialy Ionizatsii i Srodstvo k Elektronu* (Chemical Bond Dissociation Energies. Ionization Potentials and Electron Affinity) (Exec. Ed. V N Kondrat'ev) (Moscow: Nauka, 1974)
24. Gochelashvili K S et al. *JETP Lett.* **21** 302 (1975); *Pis'ma Zh. Eksp. Teor. Fiz.* **21** 640 (1975)
25. Karlov N V, Shaitan K V *Sov. Phys. JETP* **44** 244 (1976); *Zh. Eksp. Teor. Fiz.* **71** 464 (1976)
26. Doll J D *J. Chem. Phys.* **66** 5709 (1977)
27. Basov N G et al. *JETP Lett.* **22** 102 (1975); *Pis'ma Zh. Eksp. Teor. Fiz.* **22** 221 (1975)
28. Gochelashvili K S et al. *Sov. Phys. JETP* **43** 274 (1976); *Zh. Eksp. Teor. Fiz.* **70** 531 (1976)
29. Basov N G et al. *Sov. Phys. Usp.* **20** 209 (1977); *Usp. Fiz. Nauk* **121** 427 (1977)
30. Anderson G K, Lee J T *Opt. Lett.* **3** 10 (1978)
31. Sibener S J, Lee Y T *J. Chem. Phys.* **101** 1693 (1994)
32. Sibener S J, Hislop P, in LBL Report, Pt. VII. Advanced Isotope Separation Technology (1978) p. 470
33. Eerkens J W, Isotope Technologies Report IT-88-004 (1988) pp. 3, 8, 24
34. Kim J, Eerkens J W, Miller W H *Nucl. Sci. Eng.* **156** 219 (2007)
35. Lee Y T "Isotope separation by photodissociation of Van der Waals molecules", US Patent 4,032,306 (1977)
36. Lisy J M et al. "Infrared vibrational predissociation spectroscopy of small molecular clusters", Report LBL-12981 (Berkeley, Calif.: Lawrence Berkeley Laboratory, 1981)

37. Casassa M P et al. *J. Chem. Phys.* **72** 6805 (1980)
38. Casassa M P, Bomse D S, Janda K C *J. Chem. Phys.* **74** 5044 (1981)
39. Casassa M P, Bomse D S, Janda K C *J. Phys. Chem.* **85** 2623 (1981)
40. Philippoz J M et al. *J. Phys. Chem.* **88** 3936 (1984)
41. Philippoz J M et al. *Surf. Sci.* **156** 701 (1985)
42. Philippoz J M et al. *Berich. Buns. Phys. Chem.* **89** (3) 291 (1985)
43. Van den Bergh H *Laser Optoelectron.* (3) 263 (1985)
44. Okada Y et al. *J. Mol. Struct.* **410–411** 299 (1997)
45. Kim J et al. ''Current status of the MLIS uranium enrichment process', in *Transactions of the Korean Nuclear Society Spring Meeting, Jeju, Korea, May 22, 2009*
46. Janda K C *Adv. Chem. Phys.* **60** 201 (1985)
47. Celii F G, Janda K C *Chem. Rev.* **86** 507 (1986)
48. Miller R E *J. Phys. Chem.* **90** 3301 (1986)
49. Buck U *Adv. At. Mol. Opt. Phys. D* **35** 121 (1995)
50. Gough T E, Miller R E, Scoles G *J. Chem. Phys.* **69** 1588 (1978)
51. Geraedts J et al. *Chem. Phys. Lett.* **78** 277 (1981)
52. Geraedts J, Stolte S, Reuss J *Z. Phys. A* **304** 167 (1982)
53. Geraedts J et al. *Faraday Discus. Chem. Soc.* **73** 375 (1982)
54. Geraedts J et al. *Chem. Phys. Lett.* **106** 377 (1984)
55. Heijmen B et al. *Chem. Phys.* **132** 331 (1989)
56. Liedenbaum C et al. *Z. Phys. D* **11** 175 (1989)
57. Beu T A, Takeuchi K *J. Chem. Phys.* **103** 6394 (1995)
58. Beu T A, Onoe J, Takeuchi K *J. Chem. Phys.* **106** 5910 (1997)
59. Beu T A, Okada Y, Takeuchi K *Eur. Phys. J. D* **6** 99 (1999)
60. Zellweger J-M et al. *Phys. Rev. Lett.* **52** 522 (1984)
61. Monot R et al. *Helv. Phys. Acta* **57** 271 (1984)
62. Philippoz J M et al. *Helv. Phys. Acta* **58** 871 (1985)
63. Eerkens J W *Laser Part. Beams* **16** 295 (1998)
64. Rechsteiner R et al. *Helv. Phys. Acta* **54** 282 (1981)
65. Rechsteiner R, PhD Thesis (Lausanne: EPLF, 1982) pp. 91, 92
66. Melinon P et al. *Chem. Phys.* **84** 345 (1984)
67. Lyakhov K A, Lee H J *Appl. Phys. B* **111** 261 (2013)
68. Chen C L, Chantry P J ''Isotope dissociative selective electron attachment and separation'', U.S. Patent 4,176,025 (1979)
69. Christophorou L G, Olthoff J K *Int. J. Mass Spectrom.* **205** 27 (2001)
70. Christophorou L G, Olthoff J K *Adv. Atom. Mol. Opt. Phys.* **44** 155 (2001)
71. Christophorou L G, Olthoff J K *J. Phys. Chem. Ref. Data* **29** 267 (2000)
72. Le Garrec J-L, Steinhurst D A, Smith M A *J. Chem. Phys.* **114** 8831 (2001)
73. Suess L, Parthasarathy R, Dunning F B *J. Chem. Phys.* **117** 11222 (2002)
74. Denifl G et al. *Czech. J. Phys.* **49** 383 (1999)
75. Edelson D, Griffiths J E, McAfee K B (Jr.) *J. Chem. Phys.* **37** 917 (1962)
76. Compton R N et al. *J. Chem. Phys.* **45** 4634 (1966)
77. Christophorou L G *Adv. Electron. Electron Phys.* **46** 55 (1978)
78. Henis J M S, Mabie C A *J. Chem. Phys.* **53** 2999 (1970)
79. Foster M S, Beauchamp J L *Chem. Phys. Lett.* **31** 482 (1975)
80. Klots C E *J. Chem. Phys.* **46** 1197 (1967)
81. Smith D et al. *Chem Phys. Lett.* **240** 481 (1995)
82. Braun M et al. *Eur. Phys. J. D* **35** 177 (2005)
83. Spanel P, Matejcik S, Smith D *J. Phys. B At. Mol. Opt. Phys.* **28** 2941 (1995)
84. Rosa A et al. *Chem. Phys. Lett.* **391** 361 (2004)
85. Matejcik S et al. *Int. J. Mass Spectrom.* **223–224** 9 (2003)
86. Ipolyi I, Stano M, Matejcik S *Acta Phys. Slovaca* **55** 531 (2005)
87. Hahndorf I, Illenberger E *Int. J. Mass Spectrom.* **167** 87 (1997)
88. Braun M et al. *J. Phys. B At. Mol. Opt. Phys.* **40** 659 (2007)
89. Braun M et al. *J. Phys. B At. Mol. Opt. Phys.* **42** 125202 (2009)
90. Miller T M et al. *J. Chem. Phys.* **100** 8841 (1994)
91. Stamatovic A, Schulz G J *Rev. Sci. Instrum.* **41** 423 (1970)
92. Asfandiarov N L et al. *Instrum. Exp. Tech.* **56** 76 (2013); *Prib. Tekh. Eksp.* (1) 87 (3013)
93. Lokhman V N, Makarov G N, in *Fiziko-khimicheskie Protsessy pri Selektsii Atomov i Molekul. Sb. Dokl. IX Vseross.* (*Mezhdunarod.*) *Nauchn. Konf., g. Zvenigorod, 2004* (Proc. of the IX All-Russia (Intern.) Scientific Conf. ''Physical-Chemical Processes in Selection of Atoms and Molecules'', Zvenigorod, 2004) (Ed. Yu A Kolesnikov) (Moscow: TsNIIatominform, 2004) p. 121
94. Lokhman V N, Makarov G N *Chem. Phys. Lett.* **398** 453 (2004)
95. Lokhman V N, Makarov G N *JETP* **100** 505 (2005); *Zh. Eksp. Teor. Fiz.* **127** 570 (2005)
96. Lokhman V N, Makarov G N, in *Tezisy Dokladov XVII Simpoziuma ''Sovremennaya Khimicheskaya Fizika'', Tuapse, 18–19 Sentyabrya 2005 g.* (Abstracts of the XVII Symp. ''Modern Chemical Physics'', Tuapse, 18–29 September 2005), p. 42
97. Makarov G N *Phys. Usp.* **49** 1131 (2006); *Usp. Fiz. Nauk* **176** 1155 (2006)
98. Toennies J P, Vilesov A F, Whaley K B *Phys. Today* **54** (2) 31 (2001)
99. Lugovoj E et al., in *Atomic and Molecular Beams*: *The State of the Art 2000* (Ed. R Compargue) (Berlin: Springer, 2001) p.755
100. Pi M, Mayol R, Barranco M *Phys. Rev. Lett.* **82** 3093 (1999)
101. Portner N, Toennies J P, Vilesov A F *J. Chem. Phys.* **117** 6054 (2002)
102. Casas M S et al. *Z. Phys. D* **35** 67 (1995)
103. Rama Krishna M V, Whaley K W *J. Chem. Phys.* **93** 746 (1990)
104. Sindzingre P, Klein M L, Ceperley D M *Phys. Rev. Lett.* **63** 1601 (1989)
105. Kapitza P L *Zh. Eksp. Teor. Fiz.* **11** 581 (1941)
106. Grebenev S et al. *Physica B* **280** 65 (2000)
107. Callegary C G et al. *J. Chem. Phys.* **115** 10090 (2001)
108. Stienkemeier F, Vilesov A F *J. Chem. Phys.* **115** 10119 (2001)
109. Grebenev S, Toennies J P, Vilesov A F *Science* **279** 2083 (1998)
110. Toennies J P, Vilesov A F *Annu. Rev. Phys. Chem.* **49** 1 (1998)
111. Makarov G N *Phys. Usp.* **47** 217 (2004); *Usp. Fiz. Nauk* **174** 225 (2004)
112. Dumesh B S, Surin L A *Phys. Usp.* **49** 1113 (2006); *Usp. Fiz. Nauk* **176** 1137 (2006)
113. Harms J et al. *J. Mol. Spectrosc.* **185** 204 (1996)
114. Hartmann M et al. *Phys. Rev. Lett.* **75** 1566 (1995)
115. Hartmann M et al. *J. Chem. Phys.* **110** 5109 (1999)
116. Brink D, Stringari S *Z. Phys. D* **15** 257 (1990)
117. Nauta K, Miller R E *J. Chem. Phys.* **115** 8384 (2001)
118. Madeja F et al. *J. Chem. Phys.* **116** 2870 (2002)
119. Chin S A, Krotschek E *Phys. Rev. B* **52** 10405 (1995)
120. Gspann J *Z. Phys. B* **98** 405 (1995)
121. Lewerenz M, Schilling B, Toennies J P *J. Chem. Phys.* **102** 8191 (1995)
122. Lewerenz M, Schilling B, Toennies J P *Chem. Phys. Lett.* **206** 381 (1993)
123. Makarov G N *Phys. Usp.* **46** 889 (2003); *Usp. Fiz. Nauk* **173** 913 (2003)
124. Baranov V Yu et al., in *Izotopy*: *Svoistva, Poluchenie, Primenenie* (Isotopes: Properties, Production, Applications) (Ed. V Yu Baranov) (Moscow: IzdAT, 2000) p. 357
125. Makarov G N, Petin A N *JETP Lett.* **83** 87 (2006); *Pis'ma Zh. Eksp. Teor. Fiz.* **83** 115 (2006)
126. Makarov G N, Petin A N *Chem. Phys. Lett.* **426** 464 (2006)
127. Makarov G N, Petin A N *Quantum Electron.* **36** 889 (2006); *Kvantovaya Elektron.* **36** 889 (2006)
128. Makarov G N, Petin A N *JETP* **103** 697 (2006); *Zh. Eksp. Teor. Fiz.* **130** 804 (2006)
129. Weaver J F, Carlsson A F, Madix R J *Surf. Sci. Rep.* **50** 107 (2003)
130. Asscher M, Samorjai G A, in *Atomic and Molecular Beam Methods* Vol. 2 (Ed. G Scoles) (New York: Oxford Univ. Press, 1992)
131. Comsa G, Poelsema B, in *Atomic and Molecular Beam Methods* Vol. 2 (Ed. G Scoles) (New York: Oxford Univ. Press, 1992)
132. Wodtke A M, Yuhui H, Auerbach D J *Chem. Phys. Lett.* **413** 326 (2005)
133. Gentry W R, Giese C F *Rev. Sci. Instrum.* **49** 595 (1978)
134. Makarov G N et al. *Quantum Electron.* **28** 530 (1998); *Kvantovaya Elektron.* **25** 545 (1998)
135. Apatin V M et al. *Appl. Phys. B* **29** 273 (1982)
136. Apatin V M, Makarov G N *Sov. Phys. JETP* **57** 8 (1983); *Zh. Eksp. Teor. Fiz.* **84** 15 (1983)
137. Klekamp A, Umbach E *Surf. Sci.* **249** 75 (1991)
138. Makarov G N, Thesis for Doct. Phys.-Math. Sci. (Troitsk: Institute of Spectroscopy of the USSR Academy of Sciences, 1989)
139. Fuss W *Spectrochim. Acta A* **38** 829 (1982)
140. Makarov G N *JETP Lett.* **76** 283 (2002); *Zh. Eksp. Teor. Fiz.* **84** 15 (2002)
141. Makarov G N *Chem. Phys. Lett.* **366** 490 (2002)

142. Makarov G N *JETP* **96** 241 (2003); *Zh. Eksp. Teor. Fiz.* **123** 276 (2003)
143. Burak I, Steinfeld J I, Sutton D G *J. Quant. Spectrosc. Rad. Trans.* **9** 959 (1969)
144. Makarov G N *JETP* **93** 1222 (2001); *Zh. Eksp. Teor. Fiz.* **46** 1411 (2001)
145. Makarov G N *Chem. Phys.* **290** 137 (2003)
146. Jensen R J et al. *Laser Focus* **12** (5) 51 (1976)
147. McDowell R S et al. *Spectrochim. Acta A* **42** 351 (1986)
148. Baldacchini G, Marchetti S, Montelatici V *J. Mol. Spectrosc.* **91** 80 (1982)
149. Lokhman V N, Ogurok D D, Ryabov E A *Eur. Phys. J. D* **67** 66 (2013)
150. Makarov G N, Petin A N *JETP Lett.* **93** 109 (2011); *Pis'ma Zh. Eksp. Teor. Fiz.* **93** 123 (2011)
151. Makarov G N, Ryabov E A *Vestn. Ross. Fonda. Fund. Issled.* (4) 54 (2014)
152. Makarov G N, Petin A N *JETP Lett.* **97** 76 (2013); *Pis'ma Zh. Eksp. Teor. Fiz.* **97** 82 (2013)
153. Makarov G N, Petin A N *JETP* **119** 398 (2014); *Zh. Eksp. Teor. Fiz.* **146** 455 (2014)
154. Gspann J, in *Physics of Electronic and Atomic Collisions* (Ed. S Datz) (Amsterdam: North-Holland, 1982) p. 79
155. Makarov G N, Petin A N *JETP* **107** 725 (2008); *Zh. Eksp. Teor. Fiz.* **134** 851 (2008)
156. Farges J et al. *Surf. Sci.* **106** 95 (1981)
157. Makarov G N *Phys. Usp.* **51** 319 (2008); *Usp. Fiz. Nauk* **178** 337 (2008)
158. Frenkel J *Kinetic Theory of Liquids* (Oxford: The Univ. Press, 1946); Translated from Russian: *Kineticheskaya Teoriya Zhidkostei* (Moscow–Leningrad: Izd. AN SSSR, 1945)
159. Nikol'skii B P (Ed.-in-Chief) *Spravochnik Khimika* (The Chemist's Handbook) Vol. 1 (Leningrad: Goskhimizdat, 1963)
160. Makarov G N, Petin A N *JETP Lett.* **89** 404 (2009); *Pis'ma Zh. Eksp. Teor. Fiz.* **89** 468 (2009)
161. Makarov G N, Petin A N *JETP* **110** 568 (2010); *Zh. Eksp. Teor. Fiz.* **137** 646 (2010)
162. Makarov G N, Malinovsky D E, Ogurok D D *Laser Chem.* **17** 205 (1998)
163. Makarov G N, Malinovskii D E, Ogurok D D *Tech. Phys.* **44** 31 (1999); *Zh. Tekh. Fiz.* **69** (1) 35 (1999)
164. Bekman I N "Lektsiya 5. Molekuly gazov: razmer, forma, vzaimodeistvie" ("Lecture 5. Gas molecules: size, shape, interaction"), in *Membrany v Meditsine*: *Kurs Lektsii* (The Membranes in Medicine. Lecture Course) (Moscow, 2010); http://profbeckman.narod.ru/MedMemb.files/medmemb5.pdf
165. Makarov G N *Phys. Usp.* **54** 351 (2011); *Usp. Fiz. Nauk* **181** 365 (2011)
166. Lide D R (Ed.) *Handbook of Chemistry and Physics* 74th ed. (Boca Raton: CRC Press, 1993 – 1994)
167. Smirnov B M *Phys. Usp.* **44** 1229 (2001); *Usp. Fiz. Nauk* **171** 1291 (2001)
168. Gross A, Levinne R D *J. Phys. Chem. A* **107** 9567 (2003)
169. Winkel J F et al. *J. Chem. Phys.* **103** 5177 (1995)
170. Apatin V M, Makarov G N *Appl. Phys. B* **28** 367 (1982)
171. Silex Systems Limited, http://www.silex.com.au
172. Silex: History, http://www.silex.com.au/about/history#sthash.ayd9oZyC.dpuf
173. Rousseau D, Lepingwell J "Isotopic separation by laser based technologies: safeguards related aspects", https://www.iaea.org/safeguards/symposium/2010/Documents/PapersRepository/262.pdf
174. Broad W J "Laser advances in nuclear fuel stir terror fear" *New York Times* August 20 (2011); http://www.nytimes.com/2011/08/21/science/earth/21laser.html
175. Hecht J "Laser isotope separation: Laser uranium enrichment returns from the dead" *Laser Focus World* **47** (10) 18 (2011)
176. Brumm J "GE hits milestone with laser enrichment of uranium", http://www.starnewsonline.com/article/20130528/ARTICLES/130529557
177. SILEX Uranium Enrichment, SILEX Annual Report 2014, http://www.silex.com.au
178. Jones-Bey H A *Laser Focus World* (8) 36 (2006)
179. "RNC approves GLE for test loop operation", Nuclear News, July (2008) p. 64
180. "GEH enrichment plant share bought by CAMECO", Nuclear News, August (2008) p. 157
181. "Global Laser Enrichment submits license application to build first commercial uranium enrichment plant using laser technology", Business Wire, June 30 (2009)
182. Upson S, in *IEEE Spectrum Posted 30 September 2010*; http://www.spectrum.ieee.org/energy/nuclear/laser-uranium-enrichment-makes-a-comeback
183. SILEX Process, http://www.chemeurope.com/en/encyclopedia/Silex_Process.html
184. Eerkens J W (Ed.) *Selected Papers on Laser Isotope Separation — Science and Technology* (SPIE Milestone Ser., Vol. MS 113) (Bellingham, Wash.: SPIE Optical Engineering Press, 1995) pp. 108 – 147, 257 – 687
185. Grossman E M "New enrichment technology offers detectable signatures, advocate says", Global Security Newswire, 2 August (2010); http://gsn.nti.org
186. Lyman J L "Enrichment separative capacity for SILEX", Report LA-UR-05-3786 (Los Alamos, NM: Los Alamos National Laboratory, 2005)
187. Makarov G N, Petin A N *JETP Lett.* **71** 399 (2000); *Pis'ma Zh. Eksp. Teor. Fiz.* **71** 583 (2000)
188. Makarov G N, Petin A N *Chem. Phys. Lett.* **323** 345 (2000)
189. Makarov G N, Petin A N *Quantum Electron.* **30** 738 (2000); *Kvantovaya Elektron.* **30** 738 (2000)
190. Makarov G N, Petin A N *JETP* **92** 1 (2001); *Zh. Eksp. Teor. Fiz.* **119** 5 (2001)
191. Makarov G N, Mochalov S A, Petin A N *Quantum Electron.* **31** 263 (2001); *Kvantovaya Elektron.* **31** 263 (2001)
192. Makarov G N, Petin A N *Chem. Phys.* **266** 125 (2001)
193. Apatin V M et al. *Opt. Spectrosc.* **91** 852 (2001); *Opt. Spektrosk.* **91** 910 (2001)
194. Makarov G N, Petin A N *High Energy Chem.* **36** 431 (2002); *Khim. Vys. Energ.* **36** 472 (2002)
195. Anderson J B, in *Gasdynamics, Molecular Beams and Low Density Gasdynamics* (Ed. P P Wegener) (New York: M. Dekker, 1974)
196. Landau L D, Lifshitz E M *Fluid Mechanics* (Oxford: Pergamon Press, 1987); Translated from Russian: *Gidrodinamika* (Moscow: Nauka, 1986)
197. Zel'dovich Ya B, Raizer Yu P *Physics of Shock Waves and High-Temperature Hydrodynamic Phenomena* (Mineola, NY: Dover Publ., 2002); Translated from Russian: *Fizika Udarnykh Voln i Vysokotemperaturnykh Gidrodinamicheskikh Yavlenii* (Moscow: Nauka, 1966)
198. Abramovich G N *Prikladnaya Gazovaya Dinamika* (Applied Gasdynamics) Pt. 1 (Moscow: Nauka, 1991)
199. Stupochenko Ye V, Losev S A, Osipov A I *Relaxation in Shock Waves* (New York: Springer-Verlag, 1967); Translated from Russian: *Relaksatsionnye Protsessy v Udarnykh Volnakh* (Moscow: Nauka, 1965)
200. Steinfeld J I et al. *J. Chem. Phys.* **52** 5421 (1970)
201. Weulersse J M, Genier R *Appl. Phys.* **24** 363 (1981)
202. Quick C A (Jr), Wittig C *Chem. Phys. Lett.* **48** 420 (1977)
203. Alimpiev S S et al. *Sov. J. Quantum Electron.* **13** 208 (1983); *Kvantovaya Elektron.* **10** 376 (1983)
204. Alimpiev S S *Izv. Akad. Nauk SSSR. Ser. Fiz.* **45** 1070 (1981)
205. Levin I W, Berney C V *J. Chem. Phys.* **44** 2557 (1966)
206. Christe K O et al. *Spectrochim. Acta A* **32** 1141 (1976)
207. Makarov G N, Petin A N *High Energy Chem.* **34** 384 (2000); *Khim. Vys. Energ.* **36** 472 (2000)
208. Makarov G N et al. *Chem. Phys. Rep.* **18** 539 (1999); *Khim. Fiz.* **18** (3) 71 (1999)
209. Makarov G N *Tech. Phys. Lett.* **24** 921 (1998); *Pis'ma Zh. Tekh. Fiz.* **24** (23) 35 (1998)